

RDH10, RALDH2, and CRABP2 are required components of PPAR γ -directed ATRA synthesis and signaling in human dendritic cells^[S]

Adrienn Gyöngyösi,* Istvan Szatmari,* Attila Pap,* Balazs Dezső,[†] Zoltan Pos,^{§,**} Lajos Széles,* Tamas Varga,* and Laszlo Nagy^{1,*,**††}

Department of Biochemistry and Molecular Biology,* Research Center for Molecular Medicine, University of Debrecen, Medical and Health Science Center, Debrecen, Hungary; Department of Pathology,[†] and MTA-DE “Lendület” Immunogenomics Research Group,^{††} University of Debrecen, Medical and Health Science Center, Debrecen, Hungary; MTA-SE “Lendület” Experimental and Translational Immunomics Research Group,[§] Budapest, Hungary; and Department of Genetics, Cell and Immunobiology,** Semmelweis University, Budapest, Hungary

Abstract All-*trans* retinoic acid (ATRA) has a key role in dendritic cells (DCs) and affects T cell subtype specification and gut homing. However, the identity of the permissive cell types and the required steps of conversion of vitamin A to biologically active ATRA bringing about retinoic acid receptor-regulated signaling remains elusive. Here we present that only a subset of murine and human DCs express the necessary enzymes, including RDH10, RALDH2, and transporter cellular retinoic acid binding protein (CRABP)2, to produce ATRA and efficient signaling. These permissive cell types include CD103⁺ DCs, granulocyte-macrophage colony-stimulating factor, and interleukin-4-treated bone marrow-derived murine DCs and human monocyte-derived DCs (mo-DCs). Importantly, in addition to RDH10 and RALDH2, CRABP2 also appears to be regulated by the fatty acid-sensing nuclear receptor peroxisome proliferator-activated receptor γ (PPAR γ) and colocalize in human gut-associated lymphoid tissue DCs. In our model of human mo-DCs, all three proteins (RDH10, RALDH2, and CRABP2) appeared to be required for ATRA production induced by activation of PPAR γ and therefore form a linear pathway.^[S] This now functionally validated PPAR γ -regulated ATRA producing and signaling axis equips the cells with the capacity to convert precursors to active retinoids in response to receptor-activating fatty acids and is potentially amenable to intervention in diseases involving or affecting mucosal immunity.—Gyöngyösi, A., I. Szatmari, A. Pap, B. Dezső, Z. Pos, L. Széles, T. Varga, and L. Nagy. RDH10, RALDH2, and CRABP2 are required components of PPAR γ -directed ATRA synthesis and signaling in human dendritic cells. *J. Lipid Res.* 2013. 54: 2458–2474.

Supplementary key words retinoid metabolism • retinoic acid receptor signaling • iNKT cells • lipid antigen presentation • lipid transport •

L.N. is supported by a grant from the Hungarian Scientific Research Fund (OTKA K100196) and TAMOP422_2012_0023 implemented through the New Hungary Development Plan cofinanced by the European Social Fund and the European Regional Development Fund.

Manuscript received 14 April 2013 and in revised form 3 July 2013.

Published, JLR Papers in Press, July 6, 2013
DOI 10.1194/jlr.M038984

cellular retinoic acid binding protein 2 • all-*trans* retinoic acid • peroxisome proliferator-activated receptor γ

There is an increasing appreciation that metabolic processes contribute to immune cell specification. One of the prime examples of such regulation is the generation and function of all-*trans* retinoic acid (ATRA) in several cell types of the immune system, primarily in the gut. However, it remains elusive which cell types have the capacity to produce retinoic acid, which genes are required for ATRA biosynthesis and signaling, and which factors contribute to their induction in dendritic cells (DCs).

Abbreviations: APC, antigen-presenting cell; ATRA, all-*trans* retinoic acid; BM, bone marrow; BM-DC, bone marrow-derived dendritic cell; CRABP, cellular retinoic acid binding protein; Cyp26a1, cytochrome p450 26a1; DEAB, 4-diethyl amino-benzaldehyde; DC, dendritic cell; DC-SIGN, dendritic cell-specific intercellular adhesion molecule-3-grabbing non-integrin; DI, double immunofluorescence; DSS, dextran sodium sulfate; α -GalCer, α -galactosylceramide; FABP4, fatty acid binding protein 4; GALT, gut-associated lymphoid tissue; GM-CSF, granulocyte-macrophage colony-stimulating factor; IF, immunofluorescent; IBD, inflammatory bowel disease; iDC, immature dendritic cell; IHC, immunohistochemistry; IL-4, interleukin-4; iNKT, invariant natural-killer T cell; MDR, medium-chain dehydrogenase/reductase; MLN, mesenteric lymph node; mo-DC, monocyte-derived dendritic cell; M ϕ , macrophage; NK, natural killer cell; NS, nonsilencing; NS siRNA, nonsilencing control small interfering RNA; ORF, open reading frame; PBMC, peripheral blood mononuclear cell; pDC, plasmacytoid dendritic cell; PPAR γ , peroxisome proliferator-activated receptor γ ; RAR, retinoic acid receptor; RARE, retinoic acid response element; RBP, retinol-binding protein; RBPR2, RBP4 receptor-2; RSG, rosiglitazone; RT-qPCR, quantitative RT-PCR; RXR, retinoid X receptor; SDR, short-chain dehydrogenase/reductase; siRNA, small interfering RNA; Sp-DC, splenic dendritic cell; TCR, T cell receptor; TGM2, transglutaminase 2; TLDA, TaqMan low density array.

¹To whom correspondence should be addressed.

e-mail: nagy@med.unideb.hu

^[S]The online version of this article (available at <http://www.jlr.org>) contains supplementary data in the form of six figures.

DCs have been reported to be important sentinels that play fundamental roles by capturing, processing, and presenting antigens to naive T cells in draining lymph nodes, which elicit antigen-specific immune responses. Under steady-state conditions, the CX₃CR1⁻/CD103⁺ subset continuously migrates to mesenteric lymph nodes (MLNs) and these DCs are involved in maintaining gut tolerance and homeostasis (1, 2). They promote conversion of Foxp3⁺ regulatory T cells, induce gut-homing receptors CCR9 and α4β7 expression on T and B cells, and provoke T cell-independent IgA switch in naive B cells (3–6). These intestinal immune responses are established by transforming growth factor β along with ATRA, a key cofactor for these processes (7–10). However, the mechanism of ATRA generation in DCs is not fully understood. Retinol, acquired from the diet, can be metabolized to retinal by either the members of the medium-chain dehydrogenase/reductase (MDR) superfamily or by retinol dehydrogenases from the short-chain dehydrogenase/reductase (SDR) superfamily (11). The role of RDH10 for embryonic ATRA synthesis was identified by N-ethyl-N-nitrosourea-induced forward genetic screen. These *trex* mutant/*Rdh10*-deficient animals have organ abnormalities and the missense point mutation causes an embryonic lethal phenotype at embryonic day 13.5 (12, 13).

In the second irreversible oxidative step, retinal is further converted to ATRA, catalyzed by RALDH1/ALDH1A1, RALDH2/ALDH1A2, or RALDH3/ALDH1A3 (6, 7, 14). Genetic deletion experiments have proved the physiological contribution of RALDH isoenzymes to ATRA production (15). *Raldh2*^{-/-} mice show early lethality, suggesting that this enzyme plays indispensable roles in ATRA production in embryos (16–18). Interestingly, these studies also revealed that the sites of expression of RDH10 overlap with those of RALDH2, which suggested that coexpression of both metabolic enzymes were required for ATRA generation. Finally, ATRA binds to the cellular retinoic acid binding proteins (CRABPs), which transport ATRA to the nucleus allowing the activation of retinoic acid receptors (RARs). Upon ligand activation, RARs form heterodimers with retinoid X receptors (RXRs), bind to the retinoic acid response element (RARE), and regulate the transcription of target genes (19–21).

In addition, the activation of another nuclear hormone receptor, peroxisome proliferator-activated receptor γ (PPARγ), can also modulate the immunophenotype of DCs (22). DCs treated with the PPARγ-specific ligand rosiglitazone (RSG) have enhanced lipid antigen presentation capacity (23, 24). DCs have the ability to present lipid antigens such as α-galactosylceramide (α-GalCer) via the cell surface-expressed CD1d to stimulate invariant natural-killer T cell (iNKT) cells that represent a specific T cell population with expressed Natural Killer (NK) cell lineage receptors and semi-invariant CD1d-restricted Vα24JαQ T cell receptor-α chain paired with Vβ11 in humans (25, 26). We have previously shown that PPARγ activation in monocyte-derived DCs (mo-DCs) primes them for ATRA production by the upregulation of RDH10 and RALDH2 expression. The endogenously produced ATRA then induces CD1d cell

surface protein expression and triggers intense iNKT expansion (24). However, the requirement of any of these enzymes for ATRA synthesis in DCs has not been proven yet.

The work presented here has been based on our previous results and it is a direct extension of it (24). Here we decided to comprehensively characterize the key components that are required for ATRA synthesis and transport in human mo-DCs using genetic as well as pharmacological tools to gain insights into their functional requirements. We have identified CRABP2 as a PPARγ-regulated transcript and characterized the functional contribution of RDH10, RALDH2, and CRABP2 to the enhanced transcriptional activation of ATRA target genes and also to the lipid antigen presentation capacity of mo-DCs. Using a small interfering RNA (siRNA) strategy targeting *RDH10*, *RALDH2*, or *CRABP2*, we showed that attenuated expression of each of these proteins down-modulated the PPARγ-induced *CD1d* and transglutaminase 2 (*TGM2*) expression. Furthermore, down-modulated CD1d protein level reduced α-GalCer-activated iNKT expansion in DC-T cell coculture experiments.

Furthermore, an immunohistochemistry (IHC) survey of human tissues has revealed that DCs in gut-associated lymphoid tissue (GALT) coexpress PPARγ with RDH10, RALDH2, and CRABP2 in vivo.

These data collectively suggest that RDH10 and RALDH2 along with CRABP2 represent a linear pathway, and these genes are functionally required for PPARγ-induced ATRA production and signaling in DCs ex vivo, and likely to play a similar role in vivo as well.

MATERIALS AND METHODS

Ligands

Cells were treated with vehicle control (1:1 of dimethyl sulfoxide/ethanol) or with the following ligands: RSG and GW9662 (Alexis Biochemicals), and ATRA (Sigma), AGN193109 (a gift from Roshantha A. S. Chandraratna, Allergan Inc.), AM580 (Biomol), 4-diethyl amino-benzaldehyde (DEAB) from Fluka, and α-GalCer from Kirin Brewery Ltd. (Gunma, Japan).

Generation of bone marrow-derived DCs

Bone marrow (BM) cells were isolated from the femur of C57BL/6 mice. Animals were housed under specific pathogen free conditions and the experiments were carried out under Committee of Animal Research of the University of Debrecen institutional ethical guidelines and licenses (license number: 21/2011/DEMÁB). BM cells were differentiated to bone marrow-derived DCs (BM-DCs) in RPMI 1640 culturing medium supplemented with 10% FBS (Invitrogen), 500 U/ml penicillin/streptomycin (Invitrogen), 2 mM L-glutamine (Invitrogen), 20 ng/ml granulocyte-macrophage colony-stimulating factor (GM-CSF), and 20 ng/ml interleukin-4 (IL-4) or 20 ng/ml GM-CSF alone for 9 days. Cytokine treatment was repeated at days 3 and 6. After a 9 day culturing period cells were harvested in Trizol reagent (Invitrogen) for RNA isolation.

Splenic and MLN DC separation

Pooled spleens and MLNs of male C57BL/6 mice were cut into small fragments and digested with collagenase D (Roche) for 40 min at 37°C. Solutions were filtered through a nylon mesh

and washed. Cell suspension was preincubated for 10 min at 4°C with anti-mouse CD16/CD32 mouse BD Fc Block antibody (BD Pharmingen). CD11c⁺ cells were obtained followed by anti-CD11c MACS bead (Miltenyi Biotec) separation. CD103⁺ and CD103⁻ DCs were separated by labeling the cells with anti-CD11c-APC and anti-CD103-PE (BD Pharmingen) antibodies and subsequent sorting on FACS Vantage (BD Bioscience). Cells were harvested in Trizol reagent (Invitrogen).

DC/Splenocyte coculture experiment

Pooled MLN CD103⁺ DCs were obtained as described above. We purified splenocytes from pooled spleen of BALB/c mice. Spleens were placed in a Petri dish containing RPMI 1640 medium supplemented with 10% FBS (Invitrogen). Cells were squeezed out with a glass plunger. After washing, we applied Lysing buffer (BD Pharm Lyse, BD Biosciences) against red blood cells. The cell suspension was plated in Petri dishes for 12 h to attach splenic DCs (Sp-DCs). We set the coculture experiment in 12-well plates, DC/splenocyte ratio was 1:20, corresponding to 1:10 DC:T cell ratio in 2 ml per well. After 72 h incubation at 37°C, MLN CD103⁺ DCs were separated by labeling cells with anti-CD11c-APC and anti-CD103-PE (BD Pharmingen) antibodies and subsequent sorting on FACS Vantage (BD Bioscience). Cells were harvested in Trizol reagent (Invitrogen).

Human mo-DC culture

Human monocytes (98% CD14⁺) were isolated from buffy coats of healthy volunteers, obtained with the Regional Ethical Board permit from the Regional Blood Bank, by Ficoll gradient centrifugation, followed by magnetic bead separation using anti-CD14-conjugated microbeads (Miltenyi Biotec). Monocytes were differentiated to DCs at the density of 1.5×10^6 cells/ml in RPMI 1640 medium supplemented with 10% FBS (Invitrogen), 500 U/ml penicillin/streptomycin (Invitrogen), 2 nM L-glutamine (Invitrogen), 800 U/ml GM-CSF (Gentaur Ltd.), and 500 U/ml IL-4 (Peprotech). Cells were cultured for 5 days. Ligands or vehicle control were added to the cell culture at day 0 and at day 3.

RNA interference

siRNA delivery was performed using electroporation of monocytes as described earlier (27). Monocytes were counted and resuspended in Opti-MEM (Invitrogen Life Technologies) without phenol/red at the density of 4×10^7 cells/ml. For silencing of RDH10, RALDH2, CRABP2, or fatty acid binding protein 4 (FABP4) expression, the following siRNA oligonucleotides were used: ON-TARGETplus SMART pool siRNA against human RDH10, RALDH2, CRABP2, FABP4 or ON-TARGETplus nontargeting control siRNA pool [nonsilencing (NS)] (Dharmacon, Lafayette). Non-specific (NS=scrambled control) siRNA and siFABP4 were used, that did not effect the normalized mRNA level of the examined genes. Oligonucleotides were transferred to a 4 mm cuvette (Bio-Rad) at 3 μ M final concentration. Cell suspension (100 μ l) was added, gently mixed, and incubated for 3 min at room temperature. Electroporation was performed using a Gene Pulser Xcell (Bio-Rad). Pulsing conditions were square-wave pulse, 500 V, 0.5 ms. After electroporation, cells were transferred into RPMI 1640 medium supplemented with 10% FBS (Invitrogen), 500 U/ml penicillin/streptomycin (Invitrogen), 2 nM L-glutamine, 800 U/ml GM-CSF (Gentaur Ltd.), and 500 U/ml IL-4 (Peprotech). Silencing efficiency was assessed on day 1 and day 2 post electroporation.

All siRNAs were efficient. The average siRDH10 efficiency was $48.58 \pm 8.44\%$, in the case of siRALDH2 the efficiency was $39.22 \pm 10.81\%$, and the average siCRABP2 efficiency was $44.22 \pm 9.25\%$.

Aldefluor assay

Aldehyde dehydrogenase activity of mo-DC was assessed using an ALDEFLUOR kit (StemCell Technologies). Cells were incubated at the density of 1×10^6 cells/ml in ALDEFLUOR assay buffer containing activated ALDEFLUOR substrate with or without DEAB for 40 min at 37°C. ALDEFLUOR reactive cells were monitored in FL1 channel of FACS Calibur compared with DEAB-treated control samples.

Expansion of iNKT cells

Mo-DCs were treated with 100 ng/ml of α -GalCer for 48 h to obtain α -GalCer-pulsed DCs. α -GalCer-loaded DCs (1×10^5) were cocultured with monocyte-depleted autologous peripheral blood mononuclear cells (PBMCs) (1×10^6) for 5 days in 24-well plates (1:10 DC/iNKT cell ratio). PBMCs were labeled with anti-TCR V α 24-FITC and anti-T cell receptor (TCR) V β 11-PE monoclonal antibodies (Beckman Coulter), and the double-positive iNKT population was monitored by flow cytometry using FACS Calibur. Additionally, the invariant V α 24-J α 18 (iNKT) TCR α was quantified by using real-time quantitative RT-PCR (RT-qPCR).

RT-qPCR

Total RNA was isolated from cells using Trizol reagent (Invitrogen). One hundred nanograms of total RNA were reverse transcribed with Superscript reverse transcriptase (Invitrogen) and random primers (Invitrogen). This was performed at 42°C for 2 h. Quantitative PCR was performed on LC480 platform (Roche), 40 cycles of 95°C for 10 s and 60°C for 30 s. Gene expression was quantified by the comparative threshold cycle method and normalized to human or mouse Cyclophilin A (*PPIA* and *Ppia*) expression as housekeeping gene. All PCR reactions were performed in triplicate. Values are expressed as means \pm SD.

Western blot analysis

Twenty micrograms of protein, whole cell lysate, was separated by 12.5% polyacrylamide gel and transferred to PVDF membranes (Millipore). Membranes were probed with anti-CRABP2 (208) antibody, kindly provided by Cecile R. Egly (IGBMC, INSERM, France), and then the membranes were stripped and reprobed with anti-GAPDH antibody (ab8245-100; Abcam) according to the manufacturer's recommendations.

Immunoperoxidase staining

For IHC, monocytes, vehicle-treated DCs, or RSG-treated DCs (6×10^6 cells/group) were pelleted and fixed in 4% paraformaldehyde (pH 7.3) for 24 h at 4°C. Cell blocks were then embedded in paraffin, followed by serial sectionings (4 μ m). After deparaffinization and dehydration, sections from each cell group were mounted on the same glass slides and were used for peroxidase-based indirect IHC. In brief, sections were treated with 3% H₂O₂ in methanol for 15 min at room temperature to block the endogenous peroxidase. For antigen unmasking, sections were heated in antigen-retrieving citrate buffer (pH 6.0, Dako) for 2 min at 120°C using a pressure cooker. Immunostaining of cells for CRABP2 was carried out using the standard ABC technique utilizing the primary antibody-specific biotinylated secondary antibodies (Vectastain kits, Vector Laboratories). After blocking the nonspecific binding sites, sections were incubated with the primary rabbit antibody to CRABP2 (208) at dilutions of $1 \times 1/50$ for 1 h at room temperature prior to use of the biotinylated secondary antibodies. The peroxidase-mediated color development was set up for 5 min using the VIP substrate (Vector Labs). Finally, the sections were counterstained with methyl green.

Double immunofluorescence

Double immunofluorescence (DI) was performed on formalin-fixed paraffin embedded intestinal tissue sections obtained from the archives of surgical specimens of the Department of Pathology, University of Debrecen as described earlier (28). Briefly, following antigen-retrieving and peroxidase block (see previous section), the first primary antibody was visualized with antibody-matched peroxidase-conjugated IgG followed by a tetramethyl-rhodamine-tagged tyramide (Perkin-Elmer) treatment (red fluorescence). After washing and blocking the nonspecific binding sites, sections were incubated with the second primary antibody which was then developed with the use of matched biotinylated secondary antibody (IgG[Fab]₂) and streptavidin-FITC (Vector Labs, fluorescent isothiocyanate) resulting in green fluorescence. After thorough washings, nuclear counterstaining was made with 4',6-diamidino-2-phenylindole (DAPI) containing the mounting medium (Vector Labs). To check the staining specificities, positive and negative controls were included for each immunofluorescent (IF) reaction as described earlier (28) and as indicated in the Results section.

RESULTS

ATRA biosynthesis in mouse intestinal DCs

As the first step in our studies, we have characterized the expression of the essential enzymes (Fig. 1A) of ATRA biosynthesis and signaling in cells derived from mouse in vivo or ex vivo models. Retinol is transported by retinol-binding protein (RBP), taken up by DCs via retinol binding protein receptor(s) [STRA6 and RBP4 receptor-2 (RBPR2)], and bound to the cellular retinol-binding protein (CRBP) and then serves as substrate for the members of MDR or the SDR superfamily and becomes converted to retinal (Fig. 1A). The second enzymatic step is catalyzed either by RALDH1 or RALDH2. The active metabolite is delivered to the nucleus by CRABP2 and induces the transcription of several retinoid target genes through activating the RAR/RXR heterodimers in mo-DCs. Despite extensive investigation, the components and the exact molecular regulation of this pathway are not completely characterized in either murine or human DCs.

We hypothesized that RDH10 might be the primary enzyme that initiates retinal generation in intestinal DCs and the coexpression of RDH10 and RALDH2 determines the ability of ATRA production in mucosal DCs.

To test this hypothesis, we set out to assess the steps required for ATRA production and signaling in different in vivo- and in vitro-generated DC subtypes (Fig. 1B). First we generated MLN DCs described in the Materials and Methods. The purity of the sorted population was assessed by postsort flow cytometric analysis (supplementary Fig. 1A). We measured the expression level of genes involved in ATRA synthesis and compared the gene expression levels of mRNAs between sorted populations by RT-qPCR. As expected, we could detect *Raldh2* only in CD103⁺ DCs. *Rdh10* was expressed in both populations of the MLN DCs, but at an even higher level in the CD103⁻ cells (Fig. 1C).

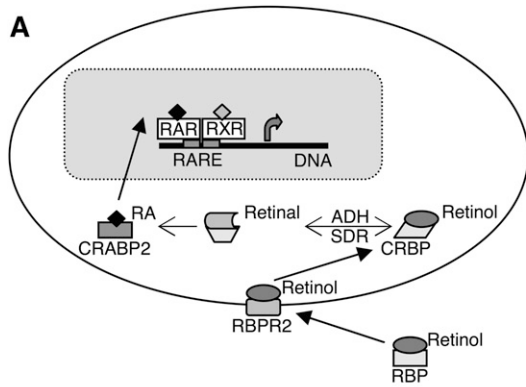
Next, we also analyzed other components of the downstream retinoid signaling pathway: we evaluated the gene expression of *Rar* and *Rxr* isoforms (supplementary Fig. 1IA). RAR/RXR heterodimers regulate retinoid target genes such as cytochrome p450 26a1 (*Cyp26a1*), which had a similar transcription pattern to the *Raldh2* gene (29). *Cyp26a1* expression itself is regulated by ATRA through two identified RAREs in the promoter of the gene, suggesting a negative feedback mechanism to control the retinoic acid concentration and active retinoid signaling in cells (30, 31). We further analyzed retinoid signaling by measuring the transcript levels of *Tgm2* and *Cd1d1*, two well-known ATRA target genes (24, 32). CD103⁺ and CD103⁻ MLN DC populations both expressed *Tgm2* and *Cd1d1*, but the normalized mRNA levels of the genes did not correlate with either *Raldh2* expression or the ATRA production capacity of the cells (Fig. 1C).

In the search for a more suitable mouse DC model for mechanistic studies, we examined ex vivo differentiated cells using TaqMan low density arrays (TLDA) in additional gene expression analyses. We differentiated GM-CSF-DC or GM-CSF+IL-4-DC from BM (Fig. 1B). To generate a negative control DC population that has no capacity for ATRA production (14), we isolated Sp-DCs from the same mouse strain (C57BL/6). We validated our BM-DC differentiation method by analyzing CD11c DC and F4/80 macrophage marker surface expression and CD11c on Sp-DCs by flow cytometry (supplementary Fig. 1B, C). GM-CSF could elicit *Raldh2* transcription, and the synergistic effect of the two cytokines was confirmed, while *Raldh2* expression in Sp-DCs was barely detectable as it was reported in case of BM-DCs (14). Next we focused on *Rdh10* in in vivo and ex vivo-generated cells and found that all DCs expressed this gene (Fig. 1D). A similar expression pattern was observed regarding *Cyp26a1*.

We compared the gene expression of all *Rar* (*a*, *b*, and *g*) and *Rxr* (*a* or *b*) expressed in mouse DCs (supplementary Fig. 1IB). We also analyzed the gene expression of *Tgm2* and *Cd1d1* in these DC populations. All DC subsets expressed *Cd1d1*, but it did not show any correlation with retinoid signaling. *Tgm2* showed a similar gene expression pattern to *Raldh2*, indicating that it could be a reliable marker of active retinoid signaling.

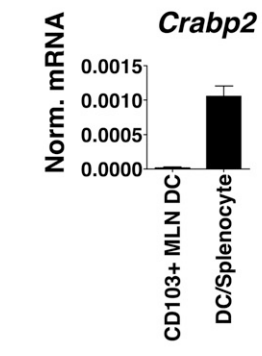
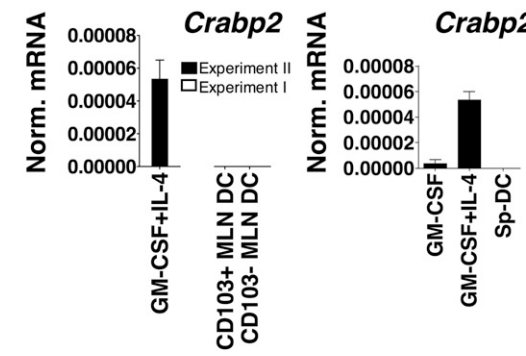
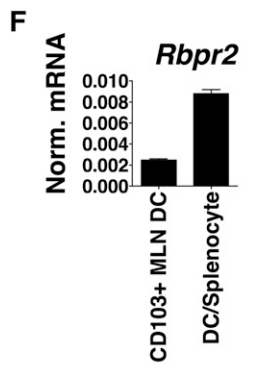
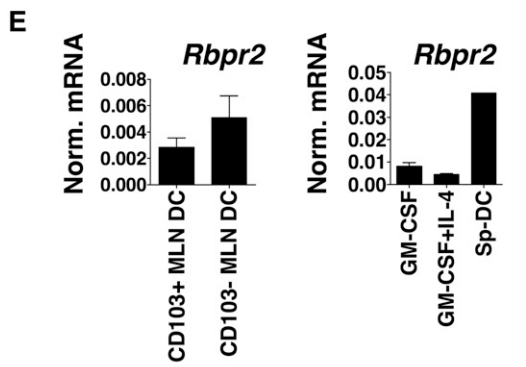
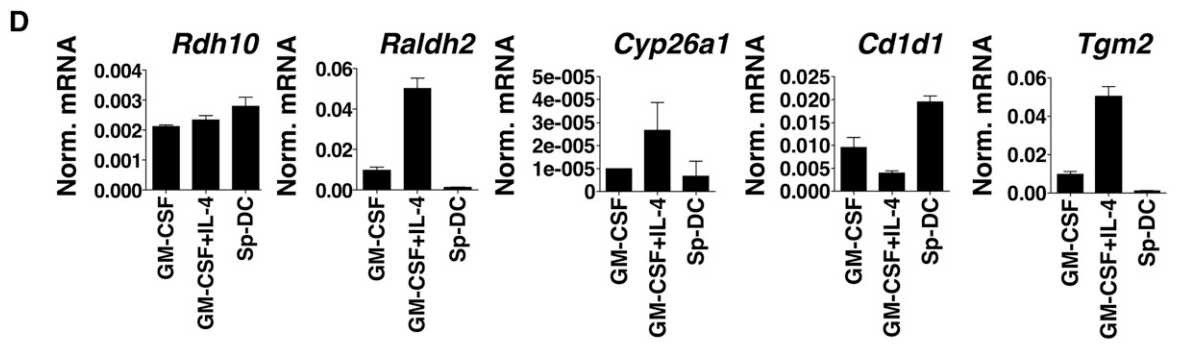
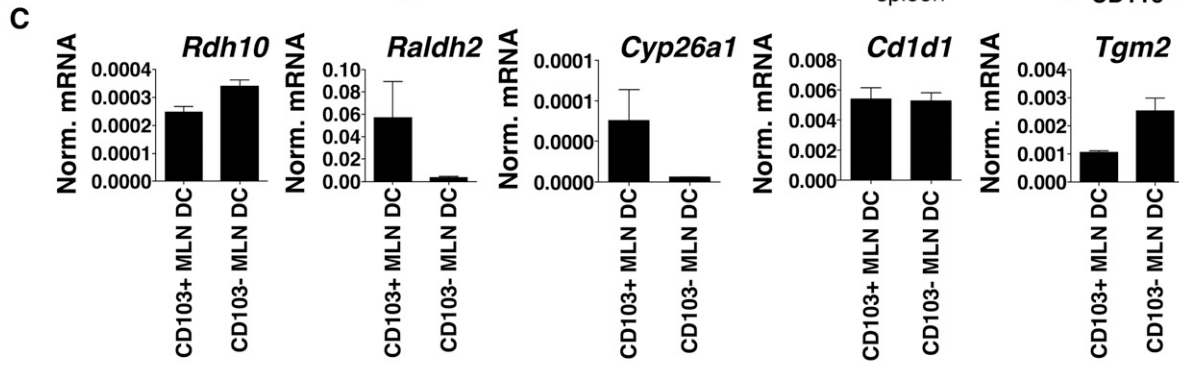
Next we assessed the expression of genes involved in retinol uptake and transport in DCs. However, the only known high-affinity receptor for retinol uptake is STRA6 (stimulated by retinoic acid-6) (33) (34). We could not detect *Strat6* gene expression in DC subsets derived from mice (data not shown). The structure of the recently identified RBPR2 is related to human and murine STRA6 (35). Therefore, we hypothesized that RBPR2 could be an alternative receptor in murine and human DCs for retinol uptake. We detected the expression of the *Rbpr2* gene in all DC subsets indicating the possibility of retinol uptake to DCs via this alternative receptor (Fig. 1E).

Unexpectedly, the transcription of the *Crabp2* gene was not detectable in in vivo subsets (Fig. 1E). The detection of *Crabp2* was successful in the case of GM-CSF or GM-CSF+IL-4 DCs in Fig. 1E; therefore, we used the measured *Crabp2*



B
MLN DCs
 C57BL/6 mice were injected with B16-Fit3L tumor cell → CD11c⁺ DCs → CD103⁺ DCs / CD103⁻ DCs

Bone marrow-derived DCs and splenic DCs
 Untreated C57BL/6 mice → bone marrow → GM-CSF-DCs / GM-CSF+IL-4-DCs
 → spleen → CD11c⁺ Sp-DCs



mRNA level in the GM-CSF+IL-4 DC sample, presented in Fig. 1D, as a technical control of the qPCR assay (labeled with Experiment II/black square in Fig. 1E; the qPCR results of the CD103⁺ and CD103⁻ MLN-DC samples are labeled with Experiment I/white square). We assessed the role of cellular interactions (T cells) using allogenic splenocytes on *Crabp2* and *Rbpr2* gene expression coculturing with ex vivo DCs. In the CD103⁺/splenocyte coculture experiment, the expression of both *Crabp2* and *Rbpr2* was induced in CD103⁺ DCs, suggesting an enhanced retinol uptake and ATRA delivery as a result of cellular, most likely T cell, interactions (Fig. 1F).

Summarizing these data, three out of five DC types (CD103⁺ MNL DCs, and GM-CSF-DCs or GM-CSF+IL-4-DCs) have a gene expression signature consistent with active ATRA biosynthesis in line with earlier published data (14). *Cyp26a1* expression with *Raldh2* appears to indicate active retinoid signaling CD103⁺ MNL DCs, and GM-CSF-DCs or GM-CSF+IL-4-DCs. We found that all DCs express the *Rdh10* gene. Based on these gene expression results, we concluded that ATRA biosynthesis is not a universal feature of DCs, and that, in line with our hypothesis, *Rdh10* expression overlaps with *Raldh2* expression suggesting that DCs expressing both enzymes are likely to have active ATRA synthesis and signaling.

Characterization of retinoid signaling in human DCs

DCs also exist in the human small intestinal MLNs. Moreover, these DCs have similar functional properties compared to CD103⁺ MLN DCs in mice (36). These data indicated that specific DCs with the ability of de novo ATRA synthesis can be present in the human body. Despite much effort and previous work (37), the human DC phenotypes are not identical and easy to match up with the ATRA-producing murine DCs. Therefore we considered using human mo-DCs for mechanistic characterization of the components of retinoid signaling by functional assays. To prove that these ex vivo cells faithfully replicate the behavior of human in vivo DCs with typical DC morphology and characteristic surface markers (23, 38–40), we examined a microarray data set and compared the gene expression pattern of mo-DCs, Langerhans cells, dermal DCs from the skin, CD1c⁺ DCs from the tonsil, and CD1c⁺ and plasmacytoid DCs (pDCs) from healthy donors (41–44). Our analysis supported the notion that mo-DCs expressed common DC markers as *CD83*, *CD1A*, *CD14*, *CD86*, *CD209*,

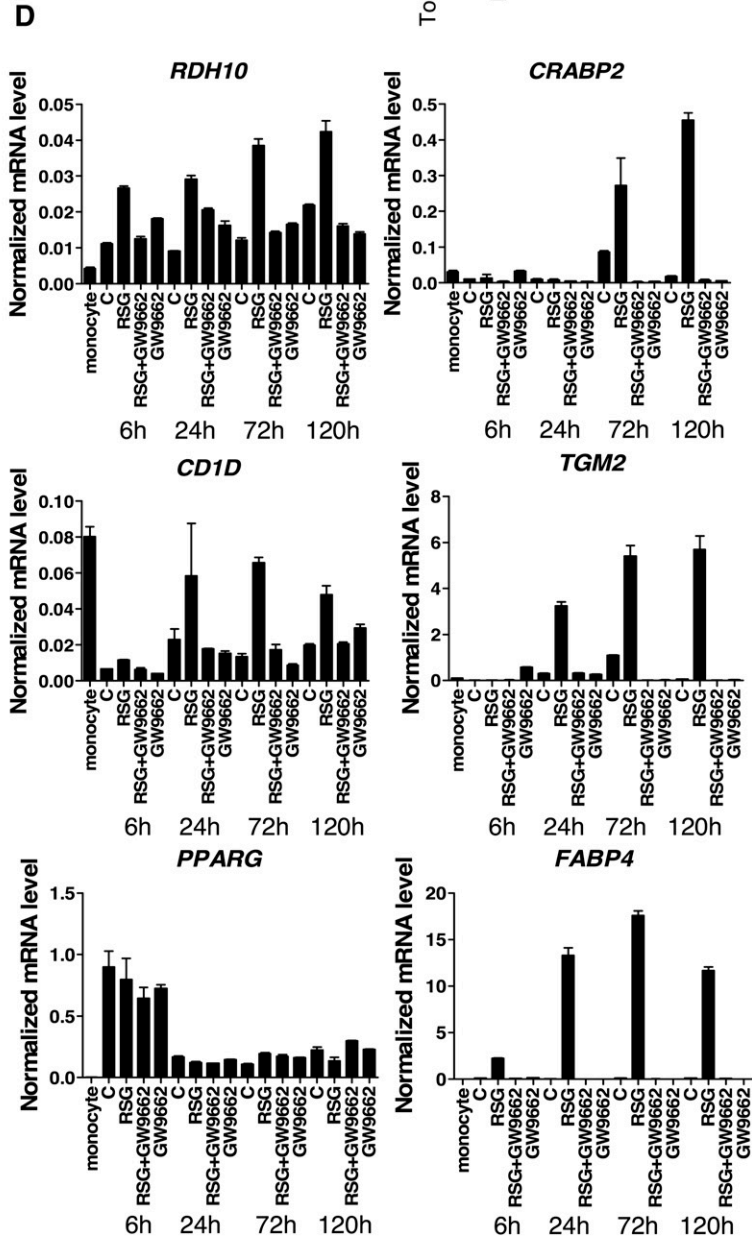
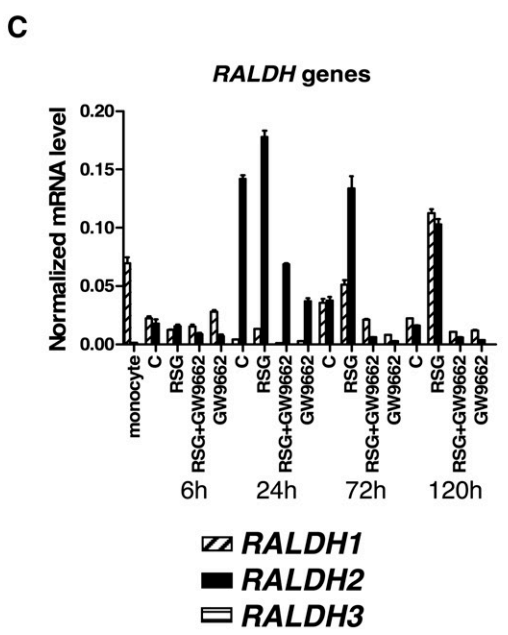
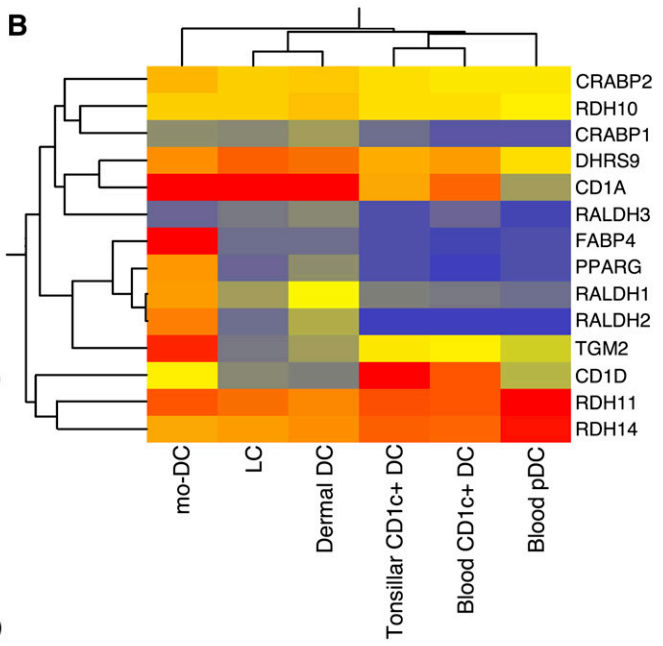
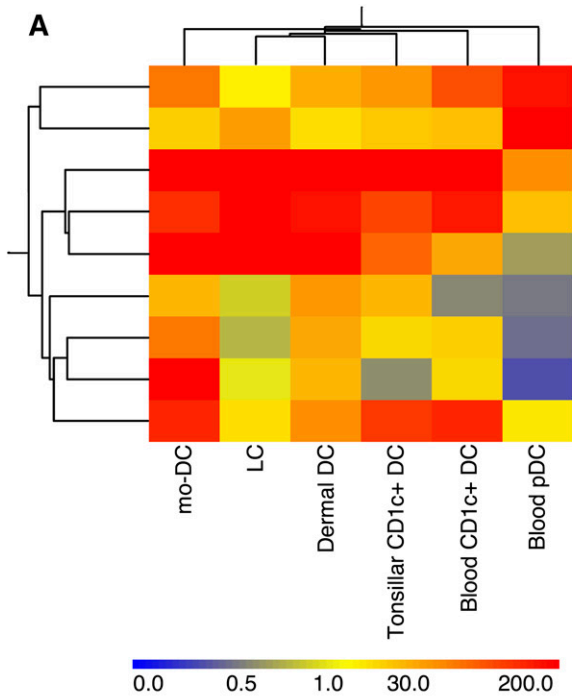
CD36, and *ILT7* pDC specific marker such as in vivo subsets (Fig. 2A). We analyzed the cell surface expression of CD14, CD209, and CD11c by FACS measurements. In line with the previously published data, monocytes were found to be CD14⁺/CD11c⁺/CD209⁻ while mo-DCs were CD14⁻/CD11c⁺/CD209⁺, and thus phenotypically resembled in vivo immature dendritic cells (iDCs) (supplementary Fig. IIIA, B).

Next, we examined the gene expression profile of a group of select genes involved specifically in ATRA biosynthesis and signaling (Fig. 2B). *RDH10*, *RDH11*, and *DHRS9* are expressed in mo-DCs (24). Both *RALDH1/ALDH1A1* and *RALDH2/ALDH1A2* are expressed at high levels in mo-DCs, while among the in vivo-generated cell types a moderate level of transcription was observed in dermal DCs only, suggesting the possibility of ATRA synthesis in that DC subtype. *RALDH3/ALDH1A3* was not expressed in these DC subsets. Among the genes encoding ATRA-transporting proteins, *CRABP1* was not expressed, while *CRABP2* was expressed ubiquitously. We also analyzed the retinoid signaling by measuring the expression of target genes: *TGM2* and *CD1D* were expressed in tonsillar CD1c⁺, blood CD1c⁺, pDC, and in mo-DCs.

Following these analyses we focused on *PPARG* and *FABP4* expression, the latter is a known marker gene of activated PPAR γ signaling (45). We have shown earlier that PPAR γ enhances ATRA production by inducing *RDH10* and *RALDH2* gene expression in mo-DCs differentiated in the presence of the synthetic PPAR γ ligand RSG (24). In line with this observation, our microarray data showed that the *PPARG* gene is expressed in mo-DCs. The detectable level of *FABP4* is likely to indicate either the presence of exogenous PPAR γ ligand in the serum or the presence of possible endogenous activators inside cells. Other in vivo-derived DC types failed to express *PPARG* or *FABP4*. This systematic analysis suggested that retinoid signaling is only active in mo-DCs that coexpress *RDH10* and *RALDH2*, and these mo-DCs have PPAR γ ligand activation connected to the retinoid signaling pathway.

Next we validated the transcriptional changes of the genes involved in ATRA production during the full differentiation period by RT-qPCR. For this, we differentiated monocytes in the presence of RSG, RSG and GW9662 (a PPAR γ antagonist), or GW9662 alone to estimate possible roles of PPAR γ in gene expression. We quantified the normalized mRNA level of *RALDH* genes at an early

Fig. 1. Characterization of the expression of genes in retinoic acid biosynthesis and signaling in murine DCs. A: The scheme of ATRA generation and retinoid signaling in DCs. Intracellularly, retinol is enzymatically converted to retinal by RDH10 and retinal is oxidized to ATRA by RALDH2. ATRA is bound to CRABPs and transported to the nucleus onto RAR/RXR heterodimers. RAR/RXR heterodimers bind to RAREs in target genes. B: MNL CD11c⁺ DCs were obtained from C57BL/6 mice and injected with B16-Flt3L tumor cells. CD103⁺ or CD103⁻ DC populations were separated based on CD103 integrin expression. Sp-DCs were isolated by CD11c magnetic beads. In vitro GM-CSF-DC and GMCSF+IL-4-DCs were differentiated from the BM of C57BL/6 mice. C: RT-qPCR analysis of genes involved in ATRA synthesis (*Rdh10*, *Raldh2*), oxidation (*Cyp26a1*), and retinoid signaling target genes (*Cd1d1*, *Tgm2*) in CD103⁺ and CD103⁻ MNL DCs. Means normalized to Cyclophilin A \pm SD. D: Comparison of gene expression pattern of genes involved in ATRA synthesis (*Rdh10*, *Raldh2*), oxidation (*Cyp26a1*), and retinoid signaling target genes (*Cd1d1*, *Tgm2*) in GM-CSF-DC and GMCSF+IL-4-DCs and Sp-DCs by the TLDA method. Means normalized to Cyclophilin A \pm SD. E: RT-qPCR analysis of genes involved in retinol uptake (*Rbpr2*) and ATRA transport (*Crabp2*) in CD103⁺ and CD103⁻ MNL DCs, GM-CSF-DC, GMCSF+IL-4-DCs, and in Sp-DCs. Means normalized to Cyclophilin A \pm SD. F: Gene expression of *Rbpr2* and *Crabp2* was measured by RT-qPCR in CD103⁺ MNL DCs and in CD103⁺ MNL DC/splenocyte coculture experiment. Means normalized to Cyclophilin A \pm SD.



timepoint (6 h), and as indicated at later time points (24, 72, and 120 h) (Fig. 2C). In monocytes we detected a high level of *RALDH1* that was rapidly downregulated and expressed at elevated level again on the fifth day of differentiation, indicating that *RALDH1* may be involved in retinal oxidation in fully differentiated cells. Unlike this gene, the human *RALDH2* was barely measurable at the monocyte state. After 6 h, cells expressed *RALDH2* at comparable levels to *RALDH1*. At all later time points, *RALDH2* was upregulated in the RSG-treated samples and, except for day 5, ligand treatment induced *RALDH2* transcription at similar levels as compared with *RALDH1*, suggesting that *RALDH2* not only has a dominant role in developing DCs but also acts as a metabolizing enzyme in differentiated cells. The *RALDH3* isoform was not detectable irrespective of treatments or time points. As expected, ligand treatment induced the normalized mRNA level of *RDH10* after 6 h, indicating that PPAR γ activates this gene probably via direct molecular interactions. The expression of *RDH10* in RSG-treated samples continuously increased during the entire differentiation period. We detected a similar expression pattern of *FABP4*. Interestingly, both *CRABP2* and *TGM2* genes were upregulated in RSG-treated DCs after 24 h in accordance with earlier results (24), *CD1D* was expressed at a high level in monocytes, but rapidly decreased in cultured cells. Consistent with our previous results, increased *CD1D* transcription was observed at later time points (23) in RSG-treated samples. *PPARG* was immediately induced in differentiating cells, the highest expression was detected at 6 h, and the normalized mRNA level of the gene was detectable at a somewhat lower level in DCs (Fig. 2D).

In summary, ATRA production and signaling is not a universal feature of DCs and it appears to be tightly regulated. We found evidence that ex vivo-differentiated mo-DCs express all components required for retinol to ATRA conversion and delivery, suggesting that mo-DCs have the ability for de novo ATRA synthesis and signaling. This ATRA producing capacity can be induced by the coordinate upregulation of *RDH10*, *RALDH2*, and *CRABP2*.

Transport of ATRA via CRABP2 to the nucleus is PPAR γ regulated

As a result of PPAR γ activation, we could detect elevated *RDH10* and *RALDH2* in the cytoplasm of mo-DCs, suggesting that these cells have an enhanced ability to produce retinoic acid (24).

In this part of the study, we aimed to examine whether intracellular ATRA transport could also be regulated by PPAR γ . Due to the fact that *CRABP2* was also highly

induced by PPAR γ in RSG-treated mo-DCs, we further examined and characterized its regulation (Fig. 2D). *CRABP2* delivers ATRA to the nucleus, thus enhanced expression of *CRABP2* should increase the transcriptional activity of RAR (46, 47). Simplistically, *CRABP2* would act as a co-activator-like molecule; when it is present, retinoid signaling is more efficient. As shown in Fig. 3A, PPAR γ activation profoundly induced the transcript levels of *CRABP2*. Next we examined if the gene expression changes are manifested at the protein level in mo-DCs. We found that monocytes do not express *CRABP2*, while control-treated mo-DCs have a detectable level of the protein (Fig. 3B). RSG-treated mo-DCs have a highly enhanced *CRABP2* protein level compared with control cells. This appears to be a DC-specific regulation, because monocyte-derived macrophages (M ϕ s) failed to express any *CRABP2* (Fig. 3B). We postulated that the elevated *CRABP2* expression in PPAR γ -instructed DCs might contribute to the enhanced ATRA response. By immunocytochemistry, we further confirmed the elevated *CRABP2* expression at the expression site of the delivery protein within mo-DCs. We observed elevated *CRABP2* protein expression in DCs as compared with monocytes and a strong upregulation of *CRABP2* upon RSG-treatment (Fig. 3C). Based on our immunocytochemistry and Western blot results, we concluded that PPAR γ -activated mo-DCs represent a relevant ex vivo model system that appears to be suitable to mechanistically dissect the ATRA biosynthesis and signaling pathway composed of *RDH10*, *RALDH2*, and *CRABP2* proteins that are coordinately upregulated by PPAR γ . We also realized that further investigations are needed to provide direct evidence for *CRABP2*-mediated ATRA transport to the nucleus in these cells.

PPAR γ , *RDH10*, *RALDH2*, *CRABP2*, and the ATRA-regulated *TGM2* colocalize in DCs of human GALT

In order to provide in vivo relevance to our findings, we systematically surveyed the expression of the components of ATRA biosynthesis and signaling in human tissues. We tested the expression of PPAR γ , *RDH10*, *RALDH2*, *CRABP2*, and *TGM2* in resting human GALT with no associated intestinal inflammation using in situ IF staining/DI. We chose GALT (for hematoxylin eosin section see Fig. 4B), as this is the most likely place where lipid signaling could contribute to DC differentiation and subtype specification in the gut. As shown in Fig. 4A (representing an IF image), we observed that PPAR γ could be readily detected in white adipose tissue (WAT; positive control to ensure the specificity of the antibody during IF staining). DI of resting GALT for PPAR γ (red) demonstrates that PPAR γ is in part

Fig. 2. Characterization of the expression of components of retinoic acid biosynthesis and signaling in human DCs. A: Human mo-DCs were differentiated ex vivo from monocytes in the presence of IL-4 and GM-CSF. Heat map analysis shows the gene expression patterns of DC markers in mo-DCs, Langerhans cells (LC), dermal DCs from the skin, CD1c⁺ DCs from the tonsil, and CD1c⁺ and pDCs from the blood of healthy donors. B: Heat map representation of genes participating in endogenous production, oxidation, transport of ATRA, retinoid signaling target genes, and PPAR γ -mediated pathway, comparison between mo-DCs and in vivo DC subsets. C: RT-qPCR analysis of *RALDH1*, *RALDH2*, and *RALDH3* in human mo-DCs obtained from monocytes and differentiated in the presence of DMSO/ethanol (C=Control), 2.5 μ M RSG, or 2.5 μ M RSG + 100 nM GW9662 and 100 nM GW9662. Means normalized to Cyclophilin A \pm SD. D: Kinetics of *RDH10*, *CRABP2*, *CYP26A1*, *TGM2*, *CD1D*, *PPARG*, and *FABP4* expression were determined by RT-qPCR. Monocytes were treated with DMSO/ethanol (C=Control), 2.5 μ M RSG, or 2.5 μ M RSG + 100 nM GW9662 or 100 nM GW9662 and harvested at indicated time points (monocyte, 6, 24, 72, and 120 h). Means normalized to Cyclophilin A \pm SD. One representative donor out of three.

coexpressed with Dendritic Cell-Specific Intercellular adhesion molecule-3-Grabbing Non-integrin (CD-SIGN) (green cytoplasmic, arrows) in mucosal lymphoid tissue cells that have cytoplasmic projections in a network pattern indicating DC phenotype (Fig. 4C). Interestingly, nuclear PPAR γ (red) and the cytoplasmic TGM2 proteins (green) show co-expression in similar cells of GALT exhibiting cytoplasmic green projection characteristic of DC elements, comparable with the staining pattern as seen for PPAR γ -DC-SIGN of image C. Therefore, these cells coexpressing PPAR γ /TGM2 should represent the DC population of GALT, similarly to PPAR γ /DC-SIGN positive cells (Fig. 4D). These data indicate that in resting lymphoid tissues some of the PPAR γ -positive DCs express TGM2 simultaneously, suggesting that PPAR γ might regulate ATRA-dependent transcription in vivo as well. On the other hand, in GALT we showed that some PPAR γ (red) positive cells coexpressed RDH10 (green cytoplasm) (Fig. 4E). Similarly, we observed few PPAR γ -expressing DCs with RALDH2 and CRABP2 coexpression, respectively (Fig. 4F, G). RDH10, RALDH2, and CRABP2 (green cytoplasmic and/or nuclear) also colocalized with DC-SIGN (red cytoplasmic projections) in some mucosal DCs (Fig. 4H–J). Note that the number of RDH10-, RALDH2-, and CRABP2-positive cells are roughly the same when Fig. 4E–compared to Fig. 4H–ecting non-activated DC state in resting GALT. However, the number of PPAR γ positive cells are increased in cases of inflammatory bowel diseases (IBDs) (data not shown).

These data collectively strongly suggest that the key components of ATRA synthesis and the PPAR γ are expressed together in some of the antigen-presenting cells (APCs) of the mucosal lymphoid tissues, consistent with a previous report which demonstrated that murine intestinal DCs expressed RALDH2 (6).

Increased RALDH activity in PPAR γ -activated mo-DCs

We wanted to provide functional evidence that indeed retinoic acid biosynthesis takes place in mo-DCs. Using a sensitive and quantitative liquid chromatography-mass spectrometry (LC-MS) method, we previously reported that mo-DCs have the ability to produce ATRA by oxidation of retinal in a PPAR γ -dependent manner (24). We aimed to further investigate this result and the function of cellular RALDHs using the ALDEFLOUR staining assay that is suitable to detect enzymatic activity of RALDHs inside the cells. Cells were differentiated (as described in the Materials and Methods) in the presence of DMSO/ethanol (C=Control) RSG, or RSG+GW9662. At 120 h, the cells were divided and incubated with fluorescent ALDEFLOUR, a substrate for RALDHs, either in the absence or the presence of DEAB, a specific RALDH inhibitor. After 40 min incubation, RALDH activity was measured by flow cytometry. There were 8% RALDH positive cells among vehicle-treated DCs (Fig. 5). In the presence of RSG, the number of RALDH positive cells was increased to 40%. We noted that a much larger enzyme activity was displayed in these treated DCs than even in the positive ones in control cells. In the RSG and GW9662 cotreated sample, the RALDH activity was similar to vehicle-treated control DCs.

Next, we assessed RALDH activity in mo-DCs electroporated at monocyte stage using specific siRNAs against siRDH10, siRALDH2, and siCRABP2 and NS-scrambled control siRNA. We treated cells with DMSO/ethanol (C), RSG, and RSG+GW9662. At day five ALDEFLOUR activity was quantified. We measured lower RALDH activity only in the siRALDH2 electroporated sample (supplementary Fig. IV).

These results suggest that RALDHs are active in mo-DCs, and the enhanced ATRA production capacity of mo-DCs is PPAR γ dependent. Interestingly, we could detect heterogeneity in this respect in the RSG-mo-DC population, but the generated endogenous ATRA level is at the range of RAR activation.

PPAR γ activation induces RAR signaling/gene expression via RDH10, RALDH2, and CRABP2

Based on these data, one can hypothesize that RDH10, RALDH2, and CRABP2 might be required for PPAR γ -regulated ATRA synthesis and gene expression. Despite the murine DC results (37), the model one can test this in is the human mo-DC. PPAR γ activation leads to transcriptional activation of several RAR target genes in human mo-DCs (24). Pharmacological analysis revealed that administration of the RALDH inhibitor DEAB reduced gene expression of *CD1D* and *TGM2* upon RSG treatment, suggesting the importance of RALDH2 in PPAR γ -enhanced retinoid signaling (24). We have extended our studies by testing to determine whether the oxidizing enzymes and CRABP2 are indeed mechanistically indispensable for retinoid-regulated gene expression induced by PPAR γ . For this, we decided to use a siRNA-based approach. We delivered siRNA against *RDH10*, *RALDH2*, or *CRABP2* and *FABP4* (as a control) to CD14⁺ monocytes after cell separation via electroporation, and differentiated cells as described in the Materials and Methods. RSG was administered as indicated in Fig. 6. After 24 or 48 h of RSG treatment, we assessed the transcript level of *CD1D* and *TGM2* using RT-qPCR. We observed that PPAR γ -induced *CD1D* expression was down-modulated by all except *FABP4*-specific siRNA at both indicated time points (24 and 48 h). *TGM2* expression changes were similar at 24 h, but only *RDH10*-specific siRNA inhibited it significantly at 48 h as compared with nonsilencing control treated (NS) DCs (Fig. 6A). We quantified the gene expression of *RALDH2* by RT-qPCR. Only siRALDH2 could significantly reduce the normalized mRNA level of *RALDH2* as expected (supplementary Fig. V).

These data suggest that RDH10 is a key component of retinol conversion, and PPAR γ -mediated retinal oxidation is catalyzed by RALDH2.

In the next set of experiments, we electroporated monocytes with *RDH10*-specific siRNA and treated as described in Fig. 6B; then we measured CD1d cell surface protein expression by flow cytometry. Transient RDH10 siRNA transfection reduced CD1d levels on DCs and it was still down-regulated at day 5 post-electroporation (Fig. 6B). These results strongly suggested that PPAR γ -mediated signaling induced retinol conversion by induced RDH10 in mo-DCs. The produced retinal is oxidized to ATRA by RALDH2.

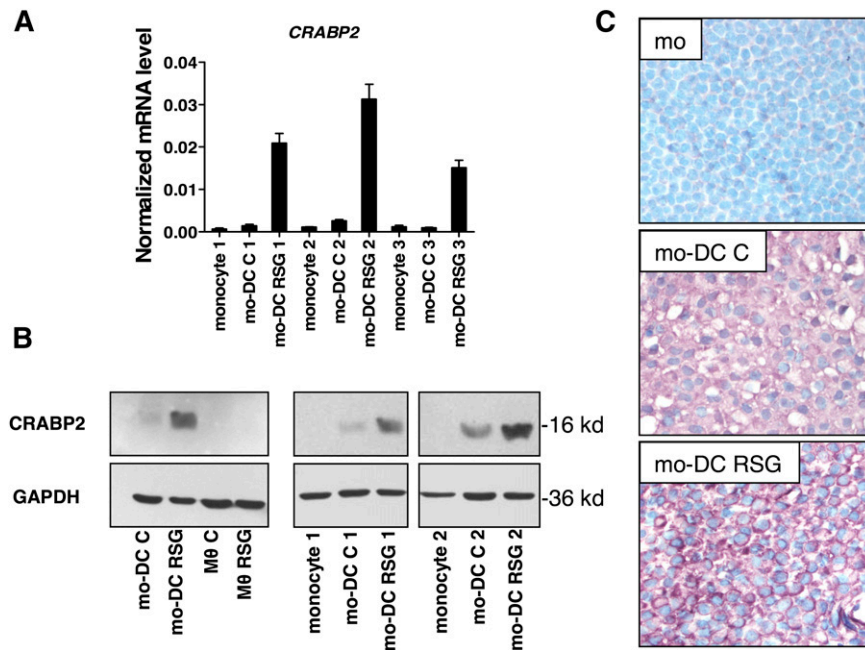


Fig. 3. Regulation of *CRABP2* expression in mo-DCs. **A:** Expression of human *CRABP2* gene was quantified by RT-qPCR. mo-DCs were obtained from three healthy donors and differentiated with IL-4 and GM-CSF for 5 days. Cells were treated at monocyte state with DMSO/ethanol (C=Control) or 2.5 μ M RSG. Means normalized to Cyclophilin A \pm SD. **B:** CRABP2 protein level was determined by Western blot. Immune cell specificity was shown as monocyte-derived macrophages (M ϕ s) failed to express CRABP2. GAPDH was used as loading control. **C:** CRABP2 expression was determined by IHC in monocytes (mo), control-treated mo-DC (mo-DC C), and RSG-treated mo-DC (mo-DC RSG) samples. CRABP2 was located in the cytoplasm of differentiated mo-DCs. Note that highest expression level for CRABP2 was observed in differentiated mo-DCs treated with RSG predominantly located in the cytoplasm. (Immune peroxidase reaction with methyl-green nuclear counterstaining; original magnification: 40 \times .)

The enhanced retinoid signaling was more effective in the presence of the CRABP2 ATRA transporter. In the nucleus, ATRA activates regulated target genes via RAR/RXR heterodimers due to integrated PPAR γ -RAR signaling.

PPAR γ -induced iNKT expansion is attenuated by RDH10, RALDH2, or CRABP2 knockdown

Next we aimed to assess the functional consequence of RDH10, RALDH2, and CRAB2 in in vitro functional assay. The lipid antigen-presenting capacity of PPAR γ -activated DCs is induced and mediated through the upregulated cell surface protein expression of CD1d protein (23, 24, 48). Human iNKT cells respond to α -GalCer, a lipid antigen restricted exclusively to CD1d molecules. First, we sought to investigate whether RDH10 can influence the PPAR γ -mediated iNKT expansion capacity of the APCs. For this, we silenced the *RDH10* gene in monocytes with *RDH10*-specific siRNA or we used a nonsilencing control siRNA (NS siRNA) as described above for Fig. 5A. Cells were differentiated to mo-DCs in the presence of DMSO/ethanol for the control-treated sample or RSG for PPAR γ activation and cells were pulsed with or without α -GalCer for 48 h and then cocultured with autologous PBMCs at a 1:10 ratio. The iNKT proliferation capacity was monitored by V α 24/V β 11 double staining. As expected, enhanced iNKT expansion was detected in RSG-treated and NS siRNA-transfected samples, while reduced iNKT cell numbers were observed in RDH10 siRNA-treated cells (Fig. 7A).

During iNKT expansion, the mRNA expression of the invariant V α 24-J α 18 (iNKT) TCR α marker gene correlates with the cell surface expression of TCR V α 24 and TCR V β 11 (48). We validated the RT-qPCR measurements on iNKT cells expanded by α -GalCer-loaded control or RSG-treated mo-DCs (Fig. 7B). Therefore, we studied the functional consequence of RDH10, RALDH2, and CRABP2 silencing on iNKT expansion by measuring V α 24-J α 18 (iNKT) TCR α gene expression as described in Fig. 6B. α -GalCer-pulsed mo-DCs have displayed enhanced V α 24-J α 18 (iNKT) TCR α gene expression further inducible by RSG administration as compared with control (NS) treated cells. Next, siRNA-treated mo-DCs were loaded with α -GalCer lipid antigen and cocultured for 5 days. As shown in Fig. 7C, siRNA against *RDH10*, *RALDH2*, and *CRABP2* enzymes reduced the normalized *TCR VA24* mRNA levels in RSG-treated samples as compared with nonsilencing control (NS) treated cells. Our data revealed significantly reduced V α 24-J α 18 (iNKT) TCR α transcription (Fig. 7C).

Based on these functional results, we could conclude that PPAR γ is acutely involved in retinoid signaling via inducing endogenous ATRA production. The primary enzyme for retinol oxidation is RDH10. The RSG-treated cells have the ability to synthesize ATRA because the coexpression of RDH10 and RALDH2 in the cells allows it. Moreover, retinoid signaling is more effective in the presence of PPAR γ -induced CRABP2 that transports ATRA to the nucleus.

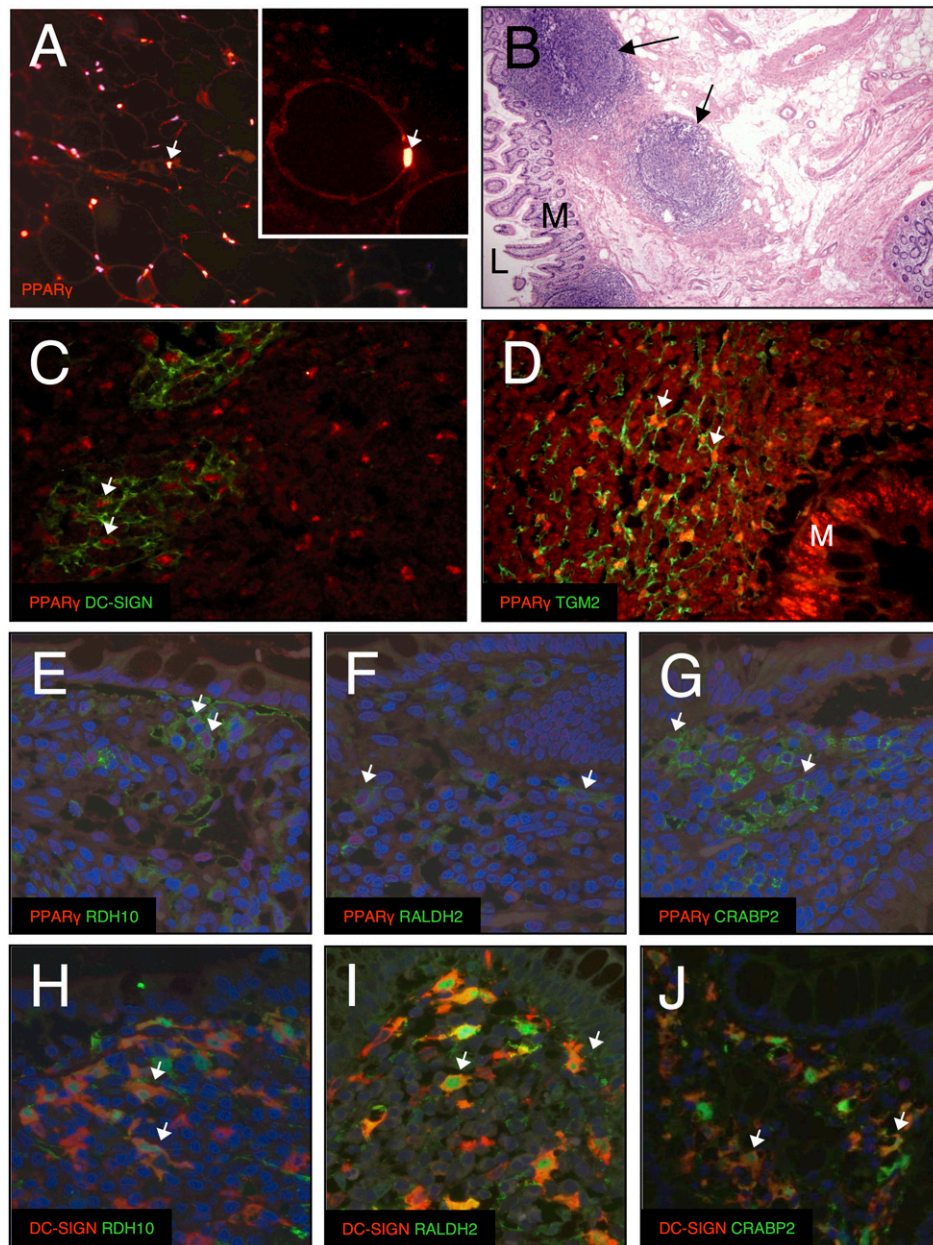


Fig. 4. DI staining analysis of ATRA biosynthesis and the putative signaling pathways along with PPAR γ expression in human GALT. A: Positive control for PPAR γ IF staining: the nuclei of white adipose tissue (WAT) cells show characteristic expression [lighting-red fluorescence (arrows) is magnified in the insert]. B: A representative area of hematoxylin eosin-stained human GALT is shown where arrows point to the mucosa-associated lymphoid tissue (M, mucosa; L, lumen). C: Using double IF, the same tissue shows that the PPAR γ protein (nuclear red fluorescence) is in part coexpressed with DC-SIGN (green cytoplasmic, arrows) in mucosal lymphoid tissue cells that have exhibiting cytoplasmic projection in a network pattern indicating DC phenotype. D: The nuclear PPAR γ (red) and the cytoplasmic TGM2 proteins (green) show coexpression in the similar cells of GALT exhibiting cytoplasmic green projection characteristic of DC elements comparable with the staining pattern as seen for the PPAR γ -DC-SIGN of image (C). E: Some of the DCs exhibiting PPAR γ (red nuclei) also express RDH10 (green cytoplasm) in resting GALT. F: Rarely, PPAR γ (red nuclei) is also colabeled with RALDH2 (green cytoplasm) in the same GALT. G: Also scattered cells with PPAR γ positivity (red nuclei) show simultaneous expression with CRABP2 (green cytoplasm, arrows) in the same GALT. H: In many DC-SIGN-positive DCs (red cytoplasm) there is a RDH10 (green nucleic and cytoplasmic) coexpression (arrows). I: DC-SIGN expressing DCs (cells with red cytoplasmic projections) may show coexpression with RALDH2 (arrow) as well (cells with green nuclei or cytoplasm). J: Few DC-SIGN-positive cells (red cytoplasm) show colocalization with CRABP2 protein (green nuclei and cytoplasm), also (arrow) indicating that CRABP2-positive cells are of DC type within resting GALT. [Except for image (B), all are DI photographs with DAPI nuclear counterstaining. Original magnifications: (A, C, D), 20 \times ; (B), 10 \times ; (E–G), 40 \times ; (H–J), 63 \times .]

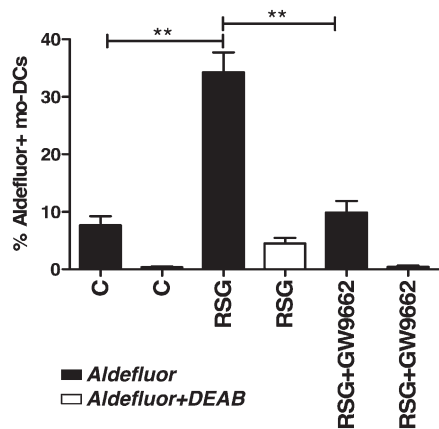


Fig. 5. RALDH activity in PPAR γ -activated mo-DCs. RALDH activity was measured utilizing ALDEFUOR kit. mo-DCs differentiated from the monocytes of healthy volunteers. DEAB-treated DCs served as negative control. The average of RALDH activity of C, RSG, and RSG+GW9662-treated mo-DCs obtained from three individual donors. **C-RSG ($P = 0.0021$), **RSG-RSG+GW9662 ($P = 0.0035$).

DISCUSSION

It is increasingly accepted that several links connect immune functions of the whole body to cellular metabolism. One of the most striking examples of such a regulatory role is the involvement of vitamin A/retinoid metabolism and ATRA production in the context of cell type specification and immune regulation. ATRA's role is primarily linked to the gut and mucosal immunity.

Intestinal homeostasis is critically controlled by the interaction between immune cells, epithelial cells, and strains of commensal bacteria. The balance between immune reactivity and tolerance under steady-state and pathogenic conditions is primarily regulated by the immunoregulatory properties of GALT-associated DCs. The main goal of our study was to systematically survey mouse and human DCs for ATRA production and signaling, and to identify and validate additional key regulatory components of endogenous ATRA synthesis in human and mouse DCs.

The endogenous ATRA generation capacity in intestinal DCs was related to the expression of intracellular RALDHs. Although previous works have demonstrated that murine DCs express several *Raldh* isoforms (7, 10, 14, 24, 49–52), the functional contribution of these isoforms to ATRA synthesis remain to be determined and the prior enzymatic step has not been evaluated in these cell types at all.

For ATRA generation, retinol is believed to be converted to retinal by members of the aldehyde dehydrogenases. Alternatively, enzymes of the SDR superfamily may also participate in this process (6). Genetic evidence that RDH10 is indispensable for embryonic retinol metabolism has been provided (12, 13) and pinpointed to this enzyme as the key mediator of this conversion. Furthermore, intracellular localization of RDH10 and RALDH2 could be correlated (16–18). These results suggested that RDH10 might be the key enzyme that could initiate retinol metabolism in intestinal DCs, and coexpression of RDH10 and RALDH2 is essentially required for the ability of mucosal CD103⁺

DCs to generate de novo ATRA. We tested this hypothesis first by using MLN DCs isolated from C57BL/6 mice, Sp-DCs from untreated mice, and ex vivo-differentiated BM-DCs in the presence of GM-CSF or GM-CSF and IL-4 (14). Using RT-qPCR and TLDA methods, we assessed that the transcription of the *Rdh10* gene was detectable in all examined DC subtypes and that the expression of *Rdh10* coincides/overlaps with *Raldh2*. We could show clear correlation between the ATRA-generating capacity of in vivo and in vitro-produced DCs and the expression of the *Cyp26a1* gene as a reliable marker for active retinoid signaling in intestinal DCs.

We also assumed that ATRA would influence the transcription of some of the known target genes identified in human DCs. Interestingly, we did not observe correlations between *Tgm2* and *Cd1d* genes and ATRA-producing capacity in in vivo subsets, particularly in the most widely characterized CD103⁺ cells.

Moreover, the gene encoding ATRA transporter *Crabp2* was also barely or not detectable in DCs of different origin. An important question is how ATRA is transported in DCs. These transport mechanisms in MLN DCs are not characterized. ATRA can be delivered to the nucleus by CRABP2 that activates retinoid signaling via RAR/RXR heterodimers or by FABP5 molecules that enhance the ligand-induced transcriptional activities of PPAR δ /RXR heterodimers (47, 53). In MLN CD103⁺ DCs CRABP2 is not expressed, but under the coculture condition the expression of *Crabp2* mRNA was induced in sorted MLN DC103⁺ DCs suggesting that T cells most likely activate *Crabp2* transcription in DCs. The signaling details of this induction require further investigations. We assessed the expression of *Crabp1* in in vivo and in vitro DC subsets as well. According to our RT-qPCR measurement, *Crabp1* is not expressed in these DCs. Based on these results, one might conclude that there might be other ATRA-delivering proteins in some of the mouse DCs.

The difference between human and murine DCs in this respect is apparent. Nuclear receptor-mediated signals might be involved in RALDH expression in intestinal DCs, leading to a specific subtype that not only stores and carries, but also produces a significant level of ATRA. However, agonists of PPAR γ did not significantly induce *Raldh2* expression in Flt3L-generated BM-DCs and purified Sp-DCs compared with the effect of IL-4 or IL-13 (14). These apparent discrepancies between the mouse and human DCs remain to be clarified. We remain of the opinion that there is not sufficient evidence to suggest that PPAR γ is able to regulate retinoid biosynthesis in murine DCs. We proved earlier that human monocytes expressed PPAR γ receptors and that the receptors are active under ex vivo culture conditions (23). Systematic microarray analyses also revealed that the activation of PPAR γ by RSG regulated the expression of genes contributing primarily to fatty acid uptake, transport, lipid storage, and attenuated lipid metabolism (43). Moreover, the PPAR γ -regulated lipid metabolic pathways could be associated with the altered immune response of DCs (23, 24, 48). PPAR γ enhanced the lipid antigen presentation capacity of DCs via CD1d

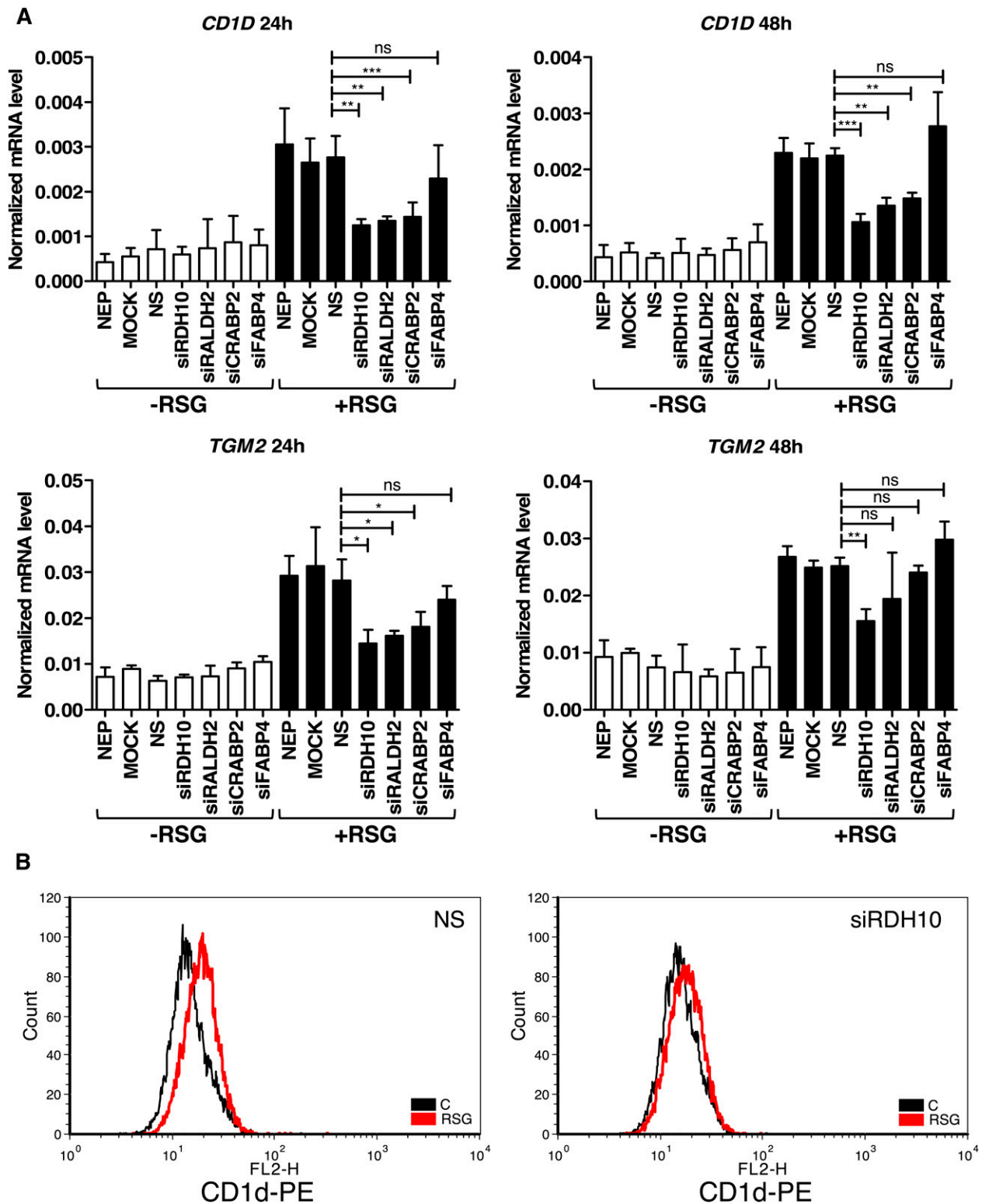


Fig. 6. Expression of RDH10, RALDH2, and CRABP2 is required for PPAR γ -induced retinoid signaling and gene expression in mo-DCs. **A:** Monocytes were electroporated with siRNA against *RDH10*, *RALDH2*, *CRABP2*, and *FABP4*. NEP, no electroporated control sample; NS, nonsilencing control sample electroporated with scrambled control siRNA. Gene expression of *CD1D* was determined by RT-qPCR. Means normalized to Cyclophilin A \pm SD; n = 3; **NS-RDH10 24 h ($P = 0.0062$); **NS-RALDH2 24 h ($P = 0.0074$); *NS-CRABP2 24 h ($P = 0.0161$), NS-FABP4 24 h ($P = 0.4082$); ***NS-RDH10 48 h ($P = 0.0005$); **NS-RALDH2 24 h ($P = 0.00713$); **NS-CRABP2 24 h ($P = 0.0014$), NS-FABP4 24 h ($P = 0.2188$). Gene expression of *TGM2* was determined by RT-qPCR. Means normalized to Cyclophilin A \pm SD; n = 3; *NS-RDH10 24 h ($P = 0.0119$), *NS-RALDH2 24 h ($P = 0.0111$), *NS-CRABP2 24 h ($P = 0.0346$), NS-FABP4 24 h ($P = 0.2539$); **NS-RDH10 48 h ($P = 0.0030$), NS-RALDH2 24 h ($P = 0.2974$), NS-CRABP2 24 h ($P = 0.3895$), NS-FABP4 24 h ($P = 0.0854$). **B:** Expression of CD1d protein on 5 day mo-DCs was measured by FACS analysis. Monocytes were electroporated with scramble control siRNA (NS) and siRNA against *RDH10* (siRDH10). mo-DCs were differentiated in the presence of DMSO/ethanol (C=Control) or 2.5 μ M RSG (RSG).

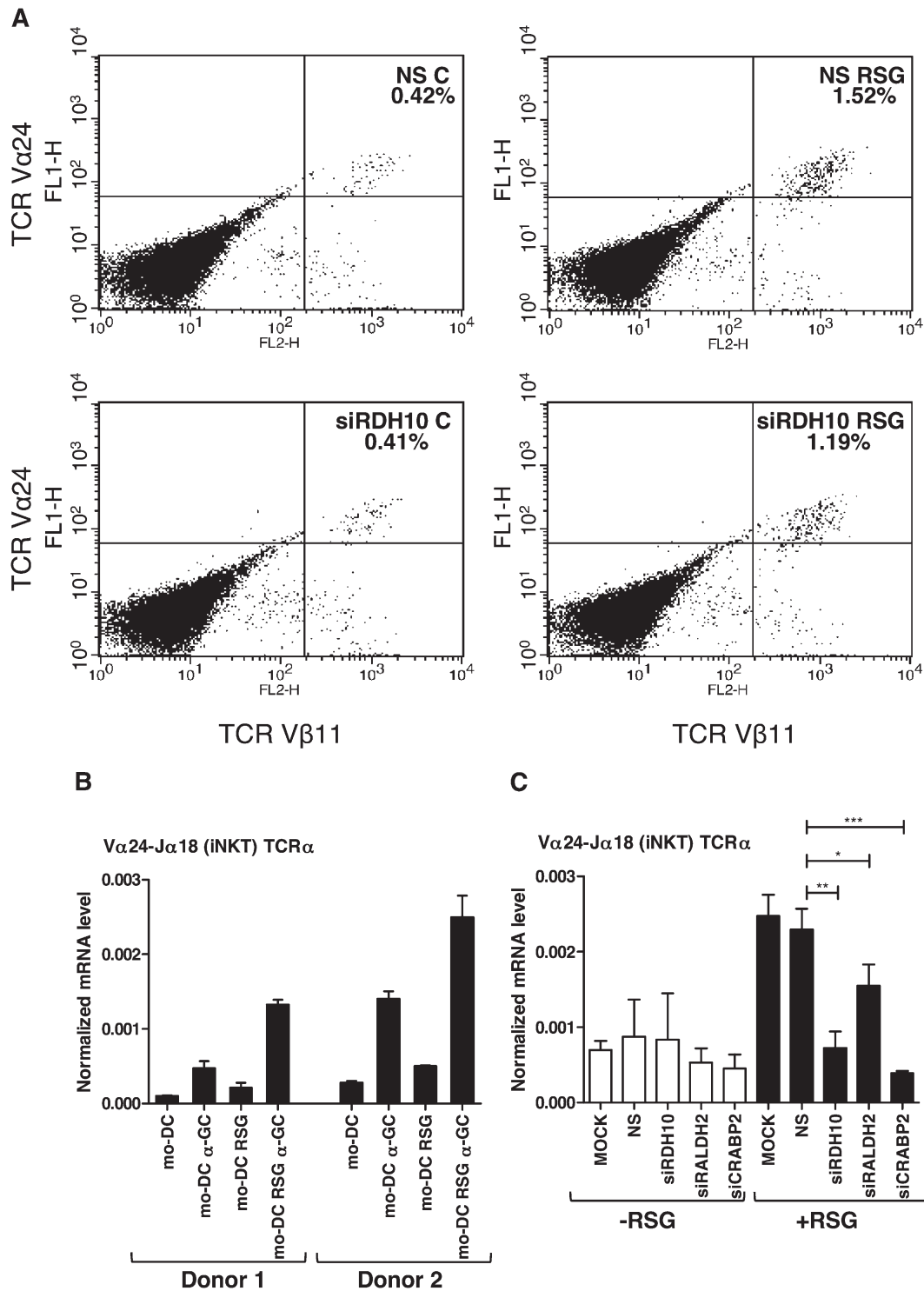


Fig. 7. RDH10 is required for PPAR γ -induced iNKT activation in mo-DCs. **A:** Expansion of iNKT cells was assessed in lipid antigen-presentation assay. Monocytes were obtained from buffy coats of healthy donors. Monocytes were electroporated with siRNA against RDH10 and scramble control siRNA (NS). Cells were differentiated in the presence of DMSO/ethanol (C=Control) or 2.5 μ M RSG (RSG) for 5 days. iNKT differentiation was detected by TCR V α 24/TCR V β 11 double staining utilizing FACS analysis. **B:** iNKT expansion was quantified by RT-qPCR. Means normalized to Cyclophilin A \pm SD. **C:** Expression of V α 24-J α 18 (iNKT) TCR α gene was quantified by RT-qPCR. Monocytes were electroporated with siRNA against RDH10, RALDH2, and CRABP2. NS, nonsilencing control sample electroporated with scrambled control siRNA. mo-DCs were differentiated in the presence of DMSO/ethanol (C=Control) or 2.5 μ M RSG (RSG) for 5 days. Means normalized to Cyclophilin A \pm SD; n = 3; **NS-RDH10 ($P = 0.0016$); *NS-RALDH2 ($P = 0.0315$); ***NS-CRABP2 ($P = 0.0003$).

molecules (23, 24, 48), which is essential for ligand presentation and recognition by the iNKTs (26, 54, 55).

In this cellular context, we have found that activation of PPAR γ initiates a transcriptional program of altered lipid metabolism in mo-DCs via induced expression of genes that are required for endogenous ATRA production (24). Importantly, we assumed that retinol is metabolized to retinal primarily by RDH10 in this process. The mRNA level of *RDH10* was increased by PPAR γ after 6 h, suggesting that this gene, like *FABP4*, could be regulated directly by PPAR γ , while the direct regulatory function and binding of PPAR γ /RXR via a response element in the *RDH10* promoter still needs to be investigated. mo-DCs express the key enzymes (RALDHs) of ATRA production. ATRA activated RAR α receptors and induced CD1d expression at mRNA and protein levels. These results suggested that transcriptional events in human mo-DCs that upregulate the *CD1d* gene are coordinately mediated by PPAR γ and RAR α receptors (23, 24).

We characterized the expression of genes responsible for retinol uptake into murine and human DCs. We could not detect *STRA6* expression in mo-DCs, the only known high-affinity receptor for RBP4 (33, 34), as we expected based on our microarray results (data not shown). We have similar results in the case of murine DCs. The structure of RBPR2, a novel retinol transporter, is related and highly conserved between human and murine *STRA6* (35). Therefore, we hypothesized that RBPR2 could be an alternative receptor in murine and human DCs for retinol uptake. We detected *Rbpr2* gene expression in a different subset of murine DCs. This gene was upregulated in MLN CD103⁺ DC under coculture conditions. The human ortholog of RBPR2 is localized at two separate sites (*RBPR2A* and *RBRP2B*) of chromosome 9's p and q arms (35). The homology between murine *Rbpr2* and the two human ortholog Open Reading Frames (ORFs) suggests the possibility that if these ORFs are transcribed, they can form functional protein on the DC surface. The expressions of human *RBPR2A* and *RBRP2B* were assessed and presented in supplementary Fig. VI. The expression of *RBPR2A* could be detected; however, this was highly donor-dependent and not altered by PPAR γ . *RBRP2B* was also expressed by DCs, but the normalized mRNA level of this fragment was much lower compared to *RBPR2A*. Additional RBP-binding assays would be required to confirm whether *RBPR2A* and *RBRP2B* can form a functional receptor on DCs.

Based on these and our previous results we chose mo-DCs as our model system to test the functional contribution of the above enzymes for ATRA synthesis and signaling. This approach proved to be successful and validated the functional requirement suggested by the gene expression studies not only at the level of gene expression, but also in T cell activating function.


An additional finding of this work is that not only ATRA synthesis can be regulated by PPAR γ but also the delivery of the active metabolite to the nucleus. We found that CRABP2 transporter protein is upregulated upon RSG-treatment, suggesting that DCs with activated PPAR γ have enhanced ATRA transport to the nucleus. We showed

earlier that RDH10 and RALDH2 proteins were expressed in mo-DCs and were upregulated upon RSG-treatment (24), and by using CRABP2-detecting IHC analysis, we confirmed that mo-DCs are a relevant ex vivo model for investigating DC ATRA producing capacity and transport. Direct evidence for CRABP-mediated ATRA transport to the nucleus requires further experimentation.

To date our knowledge is still limited about the nature of in vivo ATRA-producing APCs in the human intestinal system. GALT is the most likely place where intensive lipid absorption occurs and PPAR γ activators can be generated. Therefore it is reasonable to assume that lipid signaling could participate in DC subtype specification in these lymphoid tissues. Our IHC/DI results clearly suggested that DC-SIGN positive, GALT-associated immune cells readily express the key components of ATRA producing and signaling. In addition, PPAR γ -positive DCs coexpressed TGM2, strongly suggesting that these cells have an active retinoid signaling system and represent an in vivo relevant ATRA-producing cell type. Presumably our ex vivo mo-DCs may correspond to these in vivo DC/macrophage-like APCs.

The question of whether PPAR γ -induced ATRA generated by mucosal DCs is physiologically relevant remains to be answered. However, a link to the prevention of human IBD can be established. PPAR γ was shown to be associated with IBD in a mouse model of experimental colitis (56–58). Genetic evidence of PPAR γ -mediated protection against colon inflammation was shown in PPAR γ heterozygous mice (*Pparg*^{±/±}), and targeted disruption of the *Pparg* gene in intestinal epithelial cells enhanced the susceptibility to dextran sodium sulfate (DSS)-induced colitis (59). RSG treatment and other PPAR γ ligands attenuate the severity of colitis in both intestinal epithelial cell and macrophage-specific PPAR γ mutant mouse strains (57, 60). Due to potential side effects, the application of RSG in the treatment of IBD is not likely (61, 62). Efforts toward the discovery of a new class of PPAR γ agonist that elicits therapeutic effects against IBD with limited or no adverse side effects revealed that conjugated linoleic acid (CLA) is a safer alternative to RSG in the model of spontaneous pan-enteritis and DSS-induced colitis (63–65).

Future studies should assess the role of DC-expressed PPAR γ in IBD and potentially in other diseases. Our experimental results can be useful to design an even more effective treatment in the prevention or amelioration of ulcerative colitis and Crohn's disease.

In summary, we have established a linear relationship between RDH10, RALDH2, and CRABP2 in PPAR γ -induced ATRA synthesis and signaling that showed the requirement of these proteins. Further studies are needed to dissect the regulation of these pathways and ways to modulate their expression and activity. These new pathways could provide insight into how ATRA production could shape the immune response, and could potentially be used to treat diseases affecting mucosal immunity. 

The authors would like to acknowledge the excellent technical help of Ms. Ibolya Furtos and Marta Beladi. The authors are

indebted to Dr. Á. Lányi and the members of the Nagy laboratory for discussions and comments on the manuscript.

REFERENCES

- Johansson-Lindbom, B., M. Svensson, O. Pabst, C. Palmqvist, G. Marquez, R. Forster, and W. W. Agace. 2005. Functional specialization of gut CD103⁺ dendritic cells in the regulation of tissue-selective T cell homing. *J. Exp. Med.* **202**: 1063–1073.
- Schulz, O., E. Jaensson, E. K. Persson, X. Liu, T. Worbs, W. W. Agace, and O. Pabst. 2009. Intestinal CD103⁺, but not CX3CR1⁺, antigen sampling cells migrate in lymph and serve classical dendritic cell functions. *J. Exp. Med.* **206**: 3101–3114.
- Hammerschmidt, S. I., M. Friedrichsen, J. Boelter, M. Lyszkiewicz, E. Kremmer, O. Pabst, and R. Forster. 2011. Retinoic acid induces homing of protective T and B cells to the gut after subcutaneous immunization in mice. *J. Clin. Invest.* **121**: 3051–3061.
- Mora, J. R., M. Iwata, B. Eksteen, S. Y. Song, T. Junt, B. Senman, K. L. Otipoby, A. Yokota, H. Takeuchi, P. Ricciardi-Castagnoli, et al. 2006. Generation of gut-homing IgA-secreting B cells by intestinal dendritic cells. *Science*. **314**: 1157–1160.
- Uematsu, S., K. Fujimoto, M. H. Jang, B. G. Yang, Y. J. Jung, M. Nishiyama, S. Sato, T. Tsujimura, M. Yamamoto, Y. Yokota, et al. 2008. Regulation of humoral and cellular gut immunity by lamina propria dendritic cells expressing Toll-like receptor 5. *Nat. Immunol.* **9**: 769–776.
- Iwata, M., A. Hirakiyama, Y. Eshima, H. Kagechika, C. Kato, and S. Y. Song. 2004. Retinoic acid imprints gut-homing specificity on T cells. *Immunity*. **21**: 527–538.
- Coombes, J. L., K. R. Siddiqui, C. V. Arancibia-Carcamo, J. Hall, C. M. Sun, Y. Belkaid, and F. Powrie. 2007. A functionally specialized population of mucosal CD103⁺ DCs induces Foxp3⁺ regulatory T cells via a TGF- β and retinoic acid-dependent mechanism. *J. Exp. Med.* **204**: 1757–1764.
- Sato, A., M. Hashiguchi, E. Toda, A. Iwasaki, S. Hachimura, and S. Kaminogawa. 2003. CD11b⁺ Peyer's patch dendritic cells secrete IL-6 and induce IgA secretion from naive B cells. *J. Immunol.* **171**: 3684–3690.
- Sun, C. M., J. A. Hall, R. B. Blank, N. Bouladoux, M. Oukka, J. R. Mora, and Y. Belkaid. 2007. Small intestine lamina propria dendritic cells promote de novo generation of Foxp3⁺ T reg cells via retinoic acid. *J. Exp. Med.* **204**: 1775–1785.
- Svensson, M., B. Johansson-Lindbom, F. Zapata, E. Jaensson, L. M. Austenaa, R. Blomhoff, and W. W. Agace. 2008. Retinoic acid receptor signaling levels and antigen dose regulate gut homing receptor expression on CD8⁺ T cells. *Mucosal Immunol.* **1**: 38–48.
- Napoli, J. L. 2012. Physiological insights into all-trans-retinoic acid biosynthesis. *Biochim. Biophys. Acta.* **1821**: 152–167.
- Sandell, L. L., B. W. Sanderson, G. Moiseyev, T. Johnson, A. Mushagian, K. Young, J. P. Rey, J. X. Ma, K. Staehling-Hampton, and P. A. Trainor. 2007. RDH10 is essential for synthesis of embryonic retinoic acid and is required for limb, craniofacial, and organ development. *Genes Dev.* **21**: 1113–1124.
- Cammas, L., R. Romand, V. Fraulob, C. Mura, and P. Dolle. 2007. Expression of the murine retinol dehydrogenase 10 (Rdh10) gene correlates with many sites of retinoid signalling during embryogenesis and organ differentiation. *Dev. Dyn.* **236**: 2899–2908.
- Yokota, A., H. Takeuchi, N. Maeda, Y. Ohoka, C. Kato, S. Y. Song, and M. Iwata. 2009. GM-CSF and IL-4 synergistically trigger dendritic cells to acquire retinoic acid-producing capacity. *Int. Immunol.* **21**: 361–377.
- Kumar, S., L. L. Sandell, P. A. Trainor, F. Koentgen, and G. Duester. 2012. Alcohol and aldehyde dehydrogenases: retinoid metabolic effects in mouse knockout models. *Biochim. Biophys. Acta.* **1821**: 198–205.
- Mic, F. A., R. J. Haselbeck, A. E. Cuenca, and G. Duester. 2002. Novel retinoic acid generating activities in the lung tube and heart identified by conditional rescue of Raldh2 null mutant mice. *Development.* **129**: 2271–2282.
- Niederreither, K., V. Subbarayan, P. Dolle, and P. Chambon. 1999. Embryonic retinoic acid synthesis is essential for early mouse post-implantation development. *Nat. Genet.* **21**: 444–448.
- Niederreither, K., J. Vermot, N. Messaddeq, B. Schuhbauer, P. Chambon, and P. Dolle. 2001. Embryonic retinoic acid synthesis is essential for heart morphogenesis in the mouse. *Development.* **128**: 1019–1031.
- Chambon, P. 1996. A decade of molecular biology of retinoic acid receptors. *FASEB J.* **10**: 940–954.
- Mangelsdorf, D. J., and R. M. Evans. 1995. The RXR heterodimers and orphan receptors. *Cell.* **83**: 841–850.
- Umesono, K., V. Giguere, C. K. Glass, M. G. Rosenfeld, and R. M. Evans. 1988. Retinoic acid and thyroid hormone induce gene expression through a common responsive element. *Nature.* **336**: 262–265.
- Mangelsdorf, D. J., C. Thummel, M. Beato, P. Herrlich, G. Schutz, K. Umesono, B. Blumberg, P. Kastner, M. Mark, P. Chambon, et al. 1995. The nuclear receptor superfamily: the second decade. *Cell.* **83**: 835–839.
- Szatmari, I., P. Gogolak, J. S. Im, B. Dezso, E. Rajnavolgyi, and L. Nagy. 2004. Activation of PPAR γ specifies a dendritic cell subtype capable of enhanced induction of iNKT cell expansion. *Immunity.* **21**: 95–106.
- Szatmari, I., A. Pap, R. Ruhl, J. X. Ma, P. A. Illarionov, G. S. Besra, E. Rajnavolgyi, B. Dezso, and L. Nagy. 2006. PPAR γ controls CD1d expression by turning on retinoic acid synthesis in developing human dendritic cells. *J. Exp. Med.* **203**: 2351–2362.
- Bendelac, A., P. B. Savage, and L. Teyton. 2007. The biology of NKT cells. *Annu. Rev. Immunol.* **25**: 297–336.
- Porcelli, S. A., and R. L. Modlin. 1999. The CD1 system: antigen-presenting molecules for T cell recognition of lipids and glycolipids. *Annu. Rev. Immunol.* **17**: 297–329.
- Schaft, N., J. Dorrie, P. Thumann, V. E. Beck, I. Muller, E. S. Schultz, E. Kampgen, D. Dieckmann, and G. Schuler. 2005. Generation of an optimized polyvalent monocyte-derived dendritic cell vaccine by transfecting defined RNAs after rather than before maturation. *J. Immunol.* **174**: 3087–3097.
- Gogolak, P., B. Rethi, I. Szatmari, A. Lanyi, B. Dezso, L. Nagy, and E. Rajnavolgyi. 2007. Differentiation of CD1a- and CD1a⁺ monocyte-derived dendritic cells is biased by lipid environment and PPAR γ . *Blood.* **109**: 643–652.
- White, J. A., Y. D. Guo, K. Baetz, B. Beckett-Jones, J. Bonasoro, K. E. Hsu, F. J. Dilworth, G. Jones, and M. Petkovich. 1996. Identification of the retinoic acid-inducible all-trans-retinoic acid 4-hydroxylase. *J. Biol. Chem.* **271**: 29922–29927.
- Loudig, O., G. A. Maclean, N. L. Dore, L. Luu, and M. Petkovich. 2005. Transcriptional co-operativity between distant retinoic acid response elements in regulation of Cyp26A1 inducibility. *Biochem. J.* **392**: 241–248.
- Ray, W. J., G. Bain, M. Yao, and D. I. Gottlieb. 1997. CYP26, a novel mammalian cytochrome P450, is induced by retinoic acid and defines a new family. *J. Biol. Chem.* **272**: 18702–18708.
- Chiocca, E. A., P. J. Davies, and J. P. Stein. 1988. The molecular basis of retinoic acid action. Transcriptional regulation of tissue transglutaminase gene expression in macrophages. *J. Biol. Chem.* **263**: 11584–11589.
- Kawaguchi, R., J. Yu, J. Honda, J. Hu, J. Whitelegge, P. Ping, P. Wiita, D. Bok, and H. Sun. 2007. A membrane receptor for retinol binding protein mediates cellular uptake of vitamin A. *Science.* **315**: 820–825.
- Sun, H., and R. Kawaguchi. 2011. The membrane receptor for plasma retinol-binding protein, a new type of cell-surface receptor. *Int. Rev. Cell Mol. Biol.* **288**: 1–41.
- Alapatt, P., F. Guo, S. M. Komanetsky, S. Wang, J. Cai, A. Sargsyan, E. Rodriguez Diaz, B. T. Bacon, P. Aryal, and T. E. Graham. 2013. Liver retinol transporter and receptor for serum retinol-binding protein (RBP4). *J. Biol. Chem.* **288**: 1250–1265.
- Jaensson, E., H. Uronen-Hansson, O. Pabst, B. Eksteen, J. Tian, J. L. Coombes, P. L. Berg, T. Davidsson, F. Powrie, B. Johansson-Lindbom, et al. 2008. Small intestinal CD103⁺ dendritic cells display unique functional properties that are conserved between mice and humans. *J. Exp. Med.* **205**: 2139–2149.
- Housley, W. J., C. A. O'Connor, F. Nichols, L. Puddington, E. G. Lingenheld, L. Zhu, and R. B. Clark. 2009. PPAR γ regulates retinoic acid-mediated DC induction of Tregs. *J. Leukoc. Biol.* **86**: 293–301.
- Gosset, P., A. S. Charbonnier, P. Delerive, J. Fontaine, B. Staels, J. Pestel, A. B. Tonnel, and F. Trottein. 2001. Peroxisome proliferator-activated receptor gamma activators affect the maturation of human monocyte-derived dendritic cells. *Eur. J. Immunol.* **31**: 2857–2865.
- Sallusto, F., and A. Lanzavecchia. 1994. Efficient presentation of soluble antigen by cultured human dendritic cells is maintained by granulocyte/macrophage colony-stimulating factor plus interleukin

- 4 and downregulated by tumor necrosis factor alpha. *J. Exp. Med.* **179**: 1109–1118.
40. Thurner, B., C. Roder, D. Dieckmann, M. Heuer, M. Kruse, A. Glaser, P. Keikavoussi, E. Kampgen, A. Bender, and G. Schuler. 1999. Generation of large numbers of fully mature and stable dendritic cells from leukapheresis products for clinical application. *J. Immunol. Methods.* **223**: 1–15.
 41. Lindstedt, M., K. Lundberg, and C. A. Borrebaeck. 2005. Gene family clustering identifies functionally associated subsets of human in vivo blood and tonsillar dendritic cells. *J. Immunol.* **175**: 4839–4846.
 42. Santegoets, S. J., S. Gibbs, K. Kroeze, R. van de Ven, R. J. Scheper, C. A. Borrebaeck, T. D. de Gruijl, and M. Lindstedt. 2008. Transcriptional profiling of human skin-resident Langerhans cells and CD1a+ dermal dendritic cells: differential activation states suggest distinct functions. *J. Leukoc. Biol.* **84**: 143–151.
 43. Szatmari, I., D. Torocsik, M. Agostini, T. Nagy, M. Gurnell, E. Barta, K. Chatterjee, and L. Nagy. 2007. PPARgamma regulates the function of human dendritic cells primarily by altering lipid metabolism. *Blood.* **110**: 3271–3280.
 44. Széles, L., S. Póliska, G. Nagy, I. Szatmari, A. Szanto, A. Pap, M. Lindstedt, S. J. Santegoets, R. Rühl, B. Dezső, et al. 2010. Research resource: transcriptome profiling of genes regulated by RXR and its permissive and nonpermissive partners in differentiating monocyte-derived dendritic cells. *Mol. Endocrinol.* **24**: 2218–2231.
 45. Tontonoz, P., E. Hu, R. A. Graves, A. I. Budavari, and B. M. Spiegelman. 1994. mPPAR gamma 2: tissue-specific regulator of an adipocyte enhancer. *Genes Dev.* **8**: 1224–1234.
 46. Delva, L., J. N. Bastie, C. Rochette-Egly, R. Kraiba, N. Balitrand, G. Despouy, P. Chambon, and C. Chomienne. 1999. Physical and functional interactions between cellular retinoic acid binding protein II and the retinoic acid-dependent nuclear complex. *Mol. Cell. Biol.* **19**: 7158–7167.
 47. Dong, D., S. E. Ruuska, D. J. Levinthal, and N. Noy. 1999. Distinct roles for cellular retinoic acid-binding proteins I and II in regulating signaling by retinoic acid. *J. Biol. Chem.* **274**: 23695–23698.
 48. Nakken, B., T. Varga, I. Szatmari, L. Szeles, A. Gyongyosi, P. A. Illarionov, B. Dezso, P. Gogolak, E. Rajnavolgyi, and L. Nagy. 2011. Peroxisome proliferator-activated receptor gamma-regulated cathepsin D is required for lipid antigen presentation by dendritic cells. *J. Immunol.* **187**: 240–247.
 49. Elgueta, R., F. E. Sepulveda, F. Vilches, L. Vargas, J. R. Mora, M. R. Bono, and M. Roseblatt. 2008. Imprinting of CCR9 on CD4 T cells requires IL-4 signaling on mesenteric lymph node dendritic cells. *J. Immunol.* **180**: 6501–6507.
 50. Feng, T., Y. Cong, H. Qin, E. N. Benveniste, and C. O. Elson. 2010. Generation of mucosal dendritic cells from bone marrow reveals a critical role of retinoic acid. *J. Immunol.* **185**: 5915–5925.
 51. Iliev, I. D., I. Spadoni, E. Mileti, G. Matteoli, A. Sonzogni, G. M. Sampietro, D. Foschi, F. Caprioli, G. Viale, and M. Rescigno. 2009. Human intestinal epithelial cells promote the differentiation of tolerogenic dendritic cells. *Gut.* **58**: 1481–1489.
 52. Manicassamy, S., R. Ravindran, J. Deng, H. Oluoch, T. L. Denning, S. P. Kasturi, K. M. Rosenthal, B. D. Evavold, and B. Pulendran. 2009. Toll-like receptor 2-dependent induction of vitamin A-metabolizing enzymes in dendritic cells promotes T regulatory responses and inhibits autoimmunity. *Nat. Med.* **15**: 401–409.
 53. Schug, T. T., D. C. Berry, N. S. Shaw, S. N. Travis, and N. Noy. 2007. Opposing effects of retinoic acid on cell growth result from alternate activation of two different nuclear receptors. *Cell.* **129**: 723–733.
 54. Calabi, F., J. M. Jarvis, L. Martin, and C. Milstein. 1989. Two classes of CD1 genes. *Eur. J. Immunol.* **19**: 285–292.
 55. Kawano, T., J. Cui, Y. Koezuka, I. Toura, Y. Kaneko, K. Motoki, H. Ueno, R. Nakagawa, H. Sato, E. Kondo, et al. 1997. CD1d-restricted and TCR-mediated activation of valpha14 NKT cells by glycosylceramides. *Science.* **278**: 1626–1629.
 56. Adachi, M., R. Kurotani, K. Morimura, Y. Shah, M. Sanford, B. B. Madison, D. L. Gumucio, H. E. Marin, J. M. Peters, H. A. Young, et al. 2006. Peroxisome proliferator activated receptor gamma in colonic epithelial cells protects against experimental inflammatory bowel disease. *Gut.* **55**: 1104–1113.
 57. Bassaganya-Riera, J., K. Reynolds, S. Martino-Catt, Y. Cui, L. Hennighausen, F. Gonzalez, J. Rohrer, A. U. Benninghoff, and R. Hontecillas. 2004. Activation of PPAR gamma and delta by conjugated linoleic acid mediates protection from experimental inflammatory bowel disease. *Gastroenterology.* **127**: 777–791.
 58. Dubuquoy, L., E. A. Jansson, S. Deeb, S. Rakotobe, M. Karoui, J. F. Colombel, J. Auwerx, S. Pettersson, and P. Desreumaux. 2003. Impaired expression of peroxisome proliferator-activated receptor gamma in ulcerative colitis. *Gastroenterology.* **124**: 1265–1276.
 59. Desreumaux, P., L. Dubuquoy, S. Nütten, M. Peuchmaur, W. Englaro, K. Schoonjans, B. Derijard, B. Desvergne, W. Wahli, P. Chambon, et al. 2001. Attenuation of colon inflammation through activators of the retinoid X receptor (RXR)/peroxisome proliferator-activated receptor gamma (PPARgamma) heterodimer. A basis for new therapeutic strategies. *J. Exp. Med.* **193**: 827–838.
 60. Shah, Y. M., K. Morimura, and F. J. Gonzalez. 2007. Expression of peroxisome proliferator-activated receptor-gamma in macrophage suppresses experimentally induced colitis. *Am. J. Physiol. Gastrointest. Liver Physiol.* **292**: G657–G666.
 61. Marcy, T. R., M. L. Britton, and S. M. Blevins. 2004. Second-generation thiazolidinediones and hepatotoxicity. *Ann. Pharmacother.* **38**: 1419–1423.
 62. Nesto, R. W., D. Bell, R. O. Bonow, V. Fonseca, S. M. Grundy, E. S. Horton, M. Le Winter, D. Porte, C. F. Semenkovich, S. Smith, et al. 2003. Thiazolidinedione use, fluid retention, and congestive heart failure: a consensus statement from the American Heart Association and American Diabetes Association. October 7, 2003. *Circulation.* **108**: 2941–2948.
 63. Bassaganya-Riera, J., M. DiGuardo, M. Climent, C. Vives, A. Carbo, Z. E. Jouni, A. W. Einerhand, M. O'Shea, and R. Hontecillas. 2011. Activation of PPARgamma and delta by dietary punicalic acid ameliorates intestinal inflammation in mice. *Br. J. Nutr.* **106**: 878–886.
 64. Bassaganya-Riera, J., M. Viladomiu, M. Pedragosa, C. De Simone, A. Carbo, R. Shaykhtudinov, C. Jobin, J. C. Arthur, B. A. Corl, H. Vogel, et al. 2012. Probiotic bacteria produce conjugated linoleic acid locally in the gut that targets macrophage PPAR gamma to suppress colitis. *PLoS ONE.* **7**: e31238.
 65. Lytle, C., T. J. Tod, K. T. Vo, J. W. Lee, R. D. Atkinson, and D. S. Straus. 2005. The peroxisome proliferator-activated receptor gamma ligand rosiglitazone delays the onset of inflammatory bowel disease in mice with interleukin 10 deficiency. *Inflamm. Bowel Dis.* **11**: 231–243.